

**2D-SEISMIC REFLECTION DATA
INTERPRETATION OF LINES S96-PW-04, S96-
PW-06 AND 884-FMK-104 OF FIMKASSER AREA
PAKISTAN**



Huzaifa Athar Rasul

B.S (hons.) Geophysics

2013-2017

**DEPARTMENT OF EARTH SCIENCES
QUAID-I- AZAM UNIVERSITY
ISLAMABAD, PAKISTAN.**



“In The Name of ALLAH, the Most Merciful & Mighty”

“PAY THANKS TO ALLAH EVERY MOMENT AND GO TO EXPLORE THE
HIDDEN TREASURES, ITS ALL FOR YOUR BENEFIT”

(AL-QURAN).

CERTIFICATE

This dissertation submitted by **Huzaiifa Athar Rasul S/O MUHAMMAD Athar Rasul** is accepted in its present form by the Department of Earth Sciences, Quaid-i-Azam University Islamabad as satisfying the requirement for the award of M.Sc. degree in Geophysics.

RECOMMENDED BY

Mr. Matloob Hussain _____

(Supervisor)

Dr. Mona lisa _____

(Chairman Department of Earth Sciences)

ACKNOWLEDGEMENT

In the name of Allah, the most Beneficent, the most Merciful. All praises to Almighty Allah, the creator of universe. I bear witness that there is no God but Allah, and Holy Prophet Hazrat Muhammad (P.B.U.H) is the last messenger of Allah, whose life is a perfect model for the whole mankind till the Day of Judgment. Allah blessed me with knowledge related to Earth. Without the blessing of Allah, I could not be able to complete my work as well as to be at such a place.

I am especially indebted to my dissertation supervisor Dr. Maloob Hussain and Dr. Aamir Ali for giving me an initiative to this study. His inspiring guidance, dynamic supervision and constructive criticism, helped me to complete this work in time. I pay my thanks to whole faculty of department of Earth Sciences especially the teachers and senior students namely Muhammad Altaf and Asif changwani of Department of Earth Sciences whose valuable knowledge, assistance, cooperation and guidance enabled me to take initiative, develop and furnishing my academic carrier.

Huzaifa Athar Rasul
BS (hons.) Geophysics
2013-2017

Summary

Reservoir characterization using seismic and well data is a renowned technique within the context of Hydrocarbon exploration. This study pertains to the interpretation of seismic lines. Wireline logs and spectral decomposition for better insulation of important features at reservoir level. The study area selected for this purpose is Fimkassar.

Fimkassar is located in eastern part of Potwar basin in the Chakwal district of Punjab province. This area is surrounded by Soan syncline in the north, Jhelum fault in east, Kalabagh fault in west and Salt range in south.

The Petroleum play of Fimkassar area includes the Murree formation as a cap rock. Patala formation acts as source rock. The Chorgali and Sakesar depict the probable hydrocarbon producing reservoir.

My dissertation work is carried out on three seismic lines. The interpretation result suggest that snaked head structures are present in our area. Leading zones on contour maps are marked.

Seismic Attributes are applied for the conformation of interpretation results.

The spectral decomposition helps in identifying the bed thickness and geological discontinuities.

For Petrophysical analysis Fimkassar-02 is used for Sakesar and Chorgali. This technique tells us about the favorable zones for hydrocarbon exploration and their reservoir characteristics.

Chapter 1

INTRODUCTION

Introduction

Reservoir characterization is a process which describes us different reservoir properties using the data and helps us to get reliable reservoir models for accurate reservoir performance prediction. The most important task of reservoir engineering is to estimate the economic value and performance of reservoir in future by using proper methods (Ali et al., 2014). Reservoir characteristics can be calculated using borehole data. This data is acquired by lowering a logging formation which after travelling some distance are recorded by logging device. These reservoir characteristics are lithology, porosity and fluid saturations (Zerrouki et al., 2014).

Seismic reflection response depends on different variations existing in a rock such as lithological composition and fluid saturation (Yilmaz, 2001). Seismic data is recorded by producing seismic waves by a source and these waves travelling through the earth are recoded at specific time intervals. This data is further processed for noise for interpretation. It helps to map the reservoir and delineate oil/gas producing zones (Bacon et al., 2007). Formation tops and faults are main features to be marked. Seismic reflection method gives results with 70% accuracy (Yilmaz, 2001).

The physical properties of rocks such as volume of shale, porosity, water and Hydrocarbon saturation which are used for identifying hydrocarbon zones are obtained by petrophysics using wireline logs, core and production data (Ali et al., 2014).

Spectral decomposition is the analysis of amplitude response at different frequencies which helps in characterizing heterogeneity, fluid content and structural framework of reservoir (Julian et al., 2009). It is extremely helpful for seismic data interpretation by decomposing data into its spectral components and then reveal stratigraphic and structural details (Miao et al., 2007). It works on the principle of Fourier transform and continuous wavelet transform etc. by transforming seismic data into frequency domain (Wie, 2010).

Location of the Study Area

The Fimkassar field is located approximately 75 kilometers SW of Islamabad. Geographically, Fimkassar field is located in Chakwal district of Punjab province. Geologically it is located in

eastern part of Potwar Basin, Upper Indus basin, bounded by Soan syncline in the north, Salt Ranges in the south, Jhelum fault in east and Kalabagh fault in west. The altitude of the area is 516m. The Latitude and longitude of the study area are

Latitude 334'53.040"N

Longitude 7256'11.040"E

The location of the study area is shown in Figure 1.1.

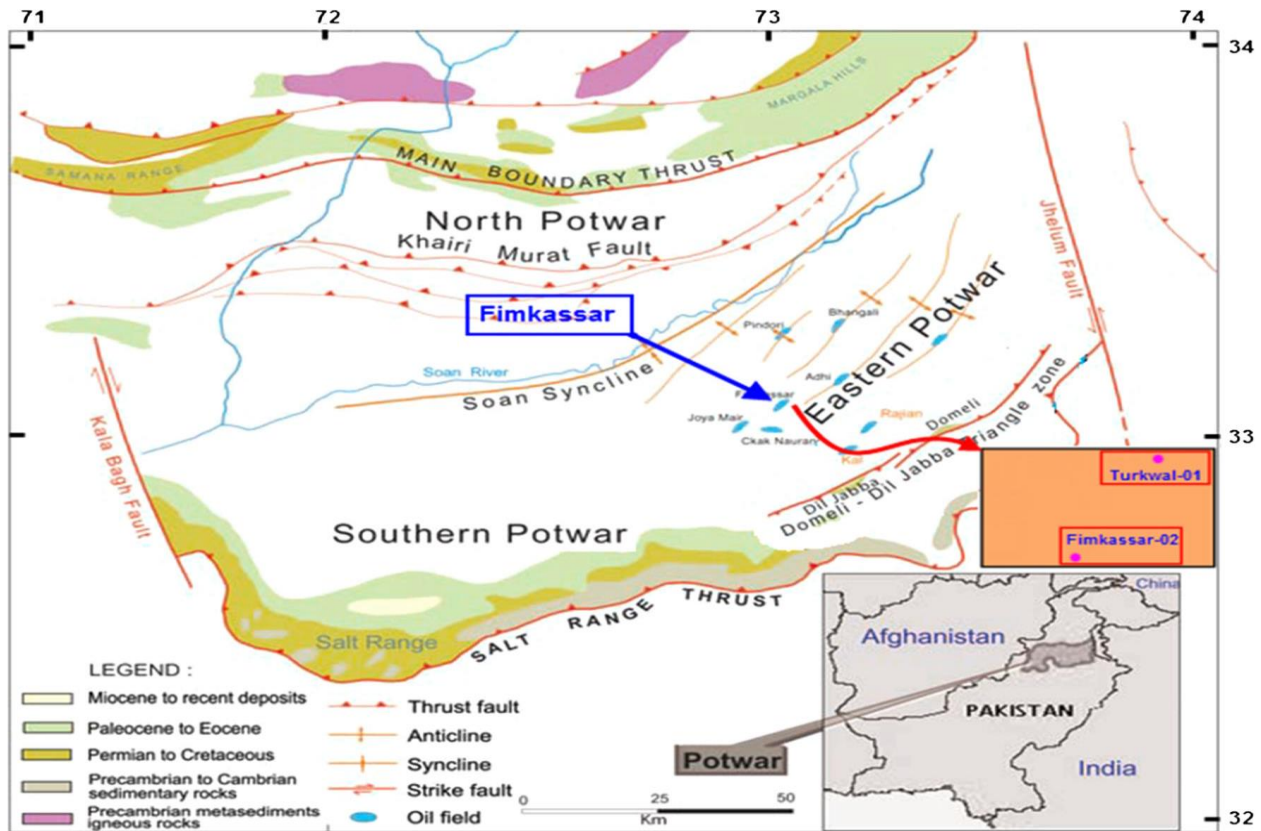


Figure 1.1 Location of study area (Amir et al., 2014).

Objectives

The main objectives of this dissertation based on interpretation of seismic section are:-

- Detailed 2D seismic interpretation identification of the structures favorable for hydrocarbon accumulation.
- Petrophysical analysis for the identification of the favorable zones hydrocarbon accumulation.
- Spectral decomposition for better visualization of important and shier features at reservoir level.

Seismic Data

12 seismic lines of the study area were provided. These lines were a mixture of strike and dip lines. The detail of these lines are given in Table 1.1. The lines which I selected are written with bold letters in the Table 1.1. A total of four wells were provided too. Two wells are used namely Turkwal-01 and Fimakssar-02. The detail of wells is given in Table 1.2.

Table 1.1

<i>Seismic Lines</i>	<i>Direction</i>	<i>Seismic Lines</i>	<i>Direction</i>
97-CP-04	Dip Line	0884-FMK-107	Dip Line
97-CP-05	Dip Line	0884-FMK-108	Dip Line
97-CP-06	Dip Line	96-PW-01	Dip Line
97-CP-07	Dip Line	96-PW-02	Dip Line
0884-FMK-103	Dip Line	96-PW-03	Dip Line
0884-FMK-104	Strike	96-PW-04	Dip Line
0884-FMK-106	Strike	96-PW-06	Dip Line

Table 1.2

<i>Well Names</i>	<i>Well Depth (m)</i>	<i>Formation tops for Sakesar (m)</i>	<i>Status of Wells</i>	<i>Discovery</i>
Fimkassar-02	3067	2946	Development	Oil & Gas
Turkwal Deep-X2	4387.7	4317	Exploratory	Abandoned
Turkwal Deep-01	4360.9	4360	Exploratory	Suspended
Turkwal-01	3245	3067	Development	Oil & Gas

Data Formats

Seismic reflection data consist of following formats:

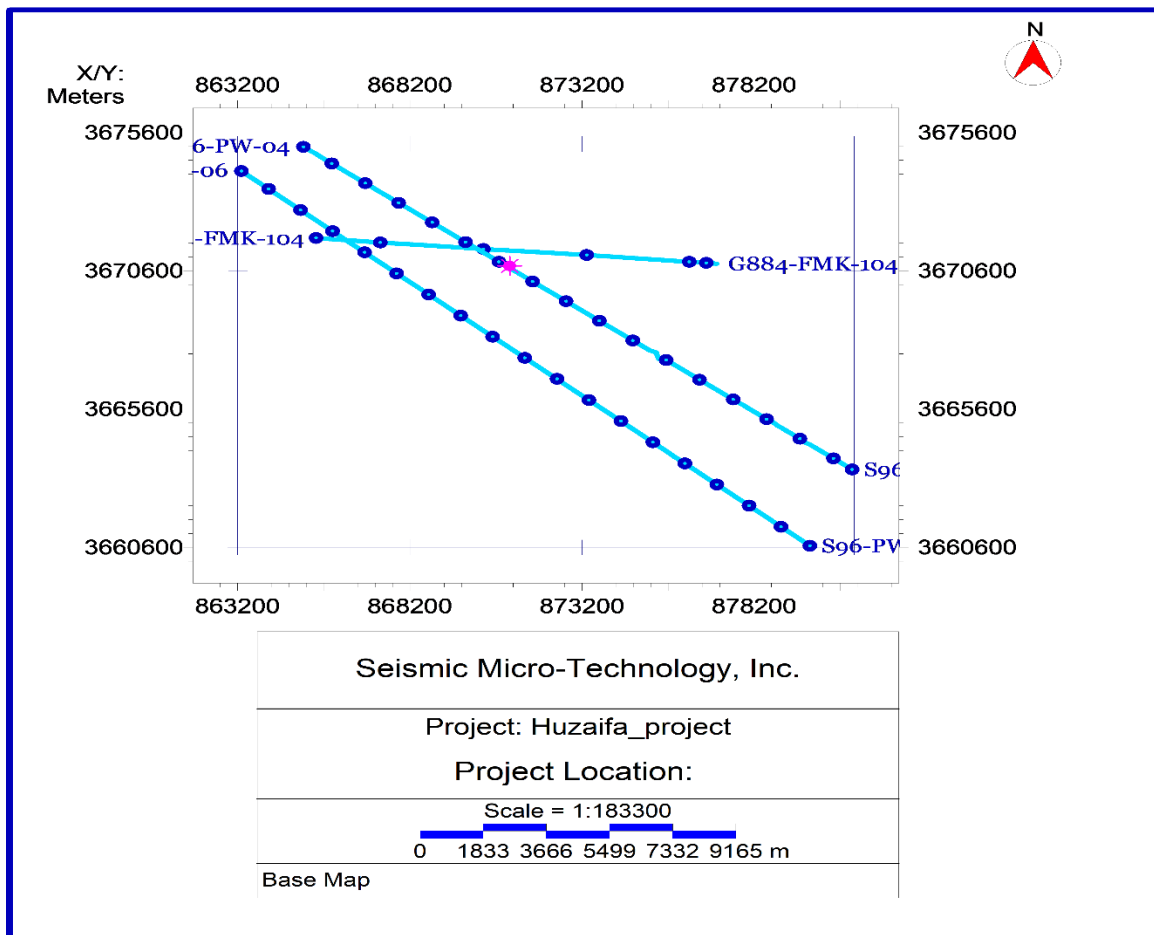
- SEG-Y
- LAS
- DAT

Software Used

IHS Kingdom 8.8 was used for the structural interpretation as well as Petrophysical analysis and Spectral decomposition.

Base Map

The base map is important component of interpretation, as it shows the spatial position of each picket of seismic section. For a Geophysicist a Base map is that which shows the orientations of seismic lines and specify points at which seismic data were acquired or simply a map which consist of number of dip and strike lines on which seismic survey is being carried out. Geophysicist typically use shot points maps, which show the orientation of seismic lines and shot points at which seismic data were required , to display interpretation of seismic data. The base map of my dissertation is shown in Figure 1.2. This base map depicts the seismic lines of my dissertation only.



Huzaifa Athar@HUZAIFAATHAR
07/11/17 23:50:18

Figure 1.2 Base map

Workflow Analysis

The Interpretation was carried forward using different techniques and steps with each step involve different processes which were performed using the software tools as mentioned above. Simplified workflow used in the dissertation is given in Figure 1.3, which provides the complete picture depicting how the dissertation has been carried.

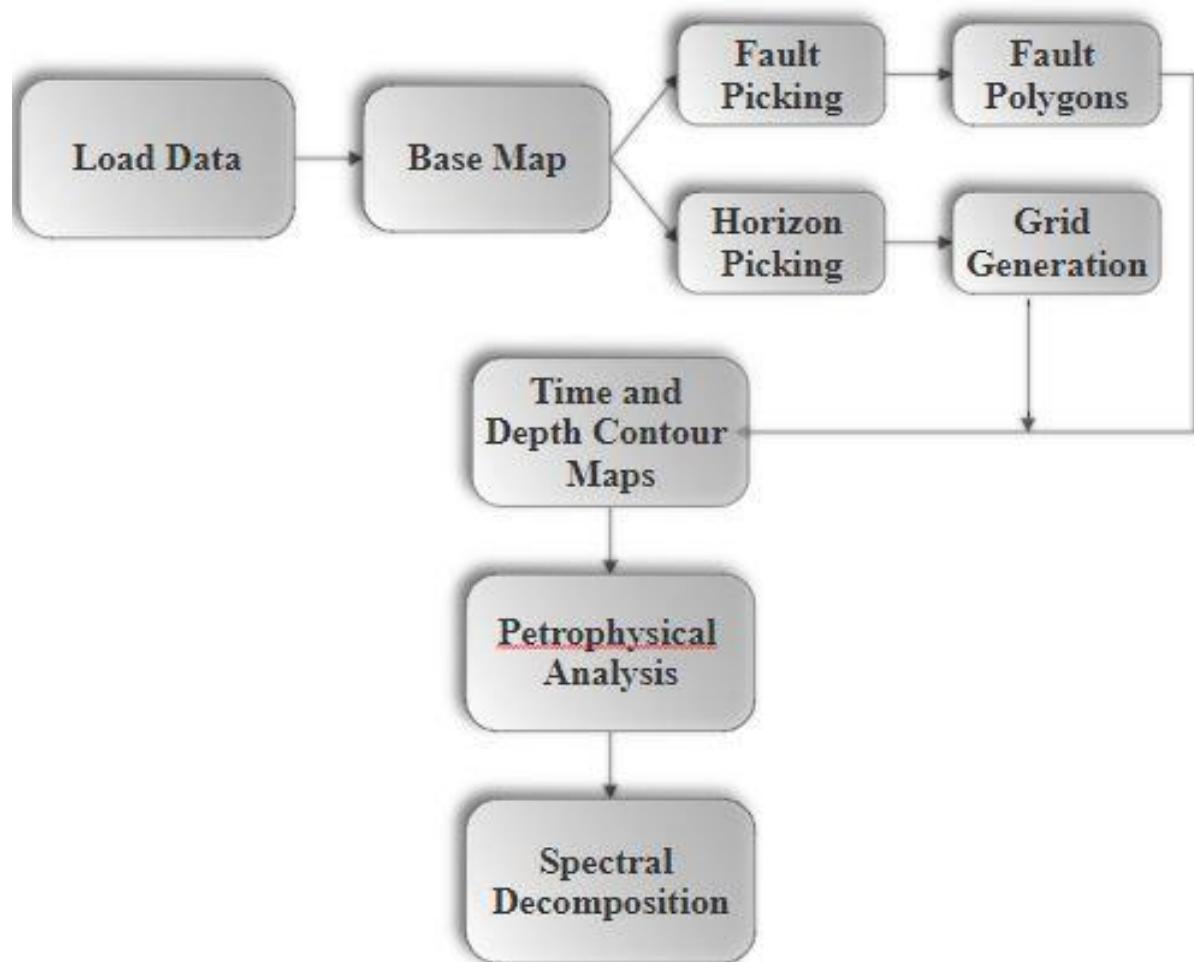


Figure 1.3 Workflow

Chapter 2

Geology and Stratigraphy of Study Area

In this chapter a brief description about the tectonic settings, structural geology and stratigraphy of Fimkassar and adjoining area of upper Indus basin is explained.

Regional Geology

In this area the formations have been compressed into fold and fault dominated structures whereas the area is dominated by overturned structures. Major thrust faults of an area dip to the north and are normally associated with south dipping conjugate back thrusts which have resulted in the formation of popup structures (Amir and Siddique, 2006). In eastern Potwar most of the folds trend NE-SW, in contrast to the EW trending folds in the central region.

Salt Range escarpment bounds the Potwar basin from south, from north bounded by Main Boundary Thrust, in east by Jhelum transform fault, and to the west by Kalabagh transform fault (Aamir and Siddiqui, 2006). Figure 2.1 shows geologic boundaries of Potwar area.

Potwar plateau is located 100 km north of the salt range and it is an elevated but nearly flat region. In north, it is bounded by Kalachitta and Margalla hills, in south salt ranges are present, Jhelum fault and Hazara Kashmir syntaxes in the east and also the Indus River and the kohat plateau to the west (Kazmi& Jan 1997). For the map of regional geology of potwar basin refer to the Figure 1.1.

Tectonics of the Study Area

In the Potwar area, the deformation appears to have occurred by south verging thrusting, with tight and occasionally overturned anticlines separated by broad synclines. The major thrust faults dip to the north and are normally associated with south dipping conjugate back thrusts, which have resulted in the formation of popup structures. The main faults detach on the regional plane of decollement i.e. Salt Range Formation (SRF).

The area is dominated by over thrust tectonics, where the formations have been compressed into fold and fault dominated structures. In eastern Potwar, most of the folds trend NE-SW, in contrast to the EW trending folds in the central region shown in Figure 2.2. Conventional imbricate thrusts, popup structures, and triangle zones are commonly developed in this area. The

wide and broad Soan syncline divides the Potwar Plateau into Northern Potwar Deformed Zone (NPDZ) and Southern Potwar Platform Zone (SPPZ). The NPDZ is more intensely deformed than the SPPZ. NPDZ is followed to the south by asymmetrical wide and broad Soan syncline, with a gently northward dipping southern flank along the salt range and a steeply dipping northern limb along NPDZ Figure 2.2. While the western NPDZ which is characterized by compressed and faulted anticlines separated by large synclines, representing the emergent thrust (Kemal, 1991).

Salt range and Domeli fore thrust systems and the Diljabba and Domeli back thrusts largely controlled the tectonic framework of eastern Potwar region. The Salt Range thrust (SRT) is an emergent thrust front with a large low angle detachment along which the Potwar Plateau has been translated southward. The Salt Range thrust defines the southernmost boundary of the Potwar area. The Salt Range thrust is a regional thrust fault and bounds the east-west trending mountainous arc and ultimately merges into Jhelum strike slip fault. The Domeli thrust is the second major thrust fault in the eastern Potwar. The Domeli thrust is a foreland verging thrust that shows a significant amount of shortening. In the eastern Potwar, some back thrusts are as large as the main thrusts.

Eastern Potwar region represents the most strongly deformed part of the Potwar fold and thrust belt. Large low angle detachment faults which accommodating more shortening than elsewhere in the Potwar fold and thrust belt. Popup structures, conventional imbricate thrusts and triangle zones are commonly developed in the area (Aamir and Siddiqui, 2006).

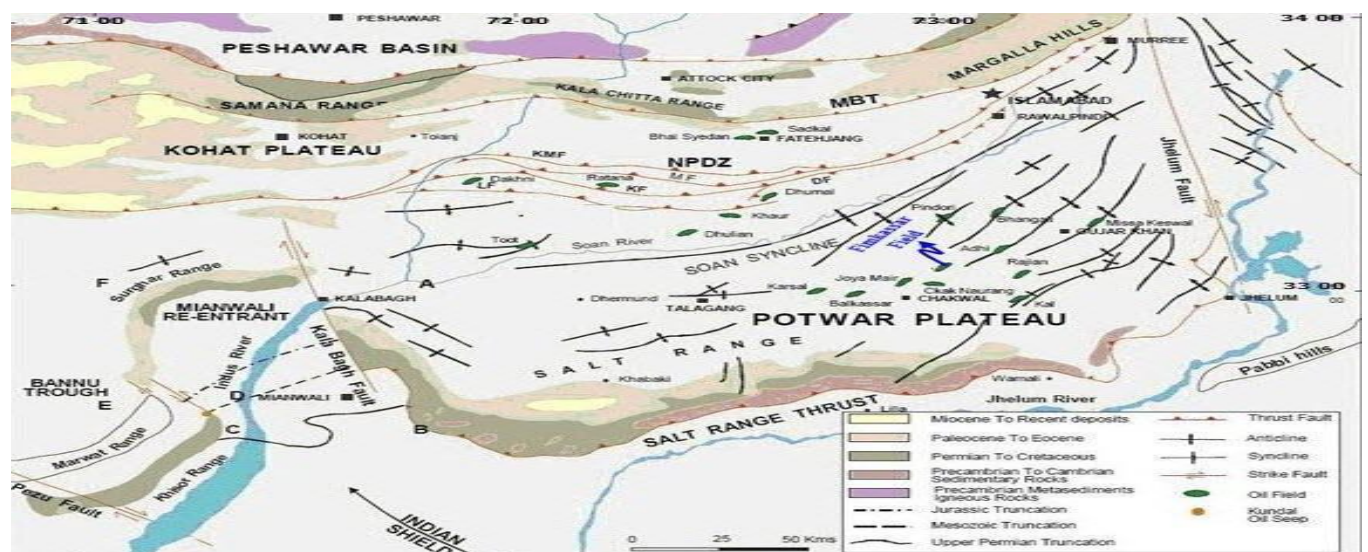


Figure 2.1 Geological and Structural Map of Potwar (Gee, 1989).

Structures in Potwar Region

By seismic interpretation following structures are observed in a potwar region

- Snake head anticlines.
- Pop-up anticlines.

Stratigraphy of Eastern Potwar Basin

The structural and stratigraphic study includes the out crop the formations at different places and the oil and water wells drilled in the area's the Salt Range-Potwar Foreland Basin. The oldest Formation of the cover sequence known to lie at the top of basement is the Eocambrian Salt Range Formation which is available as outcrop and at many places it is also in the subsurface which is confirmed from the well log data.

Area lies in the southeast Potwar sub-basin where the orientation is northeast-southwest. The rocks of Miocene-Pliocene age which are known as Nagri Formation and Chinji Formations are exposed in the core of the structure. Here thrust tectonics plays important role.

The lithological formations are lying uncomfortably over Paleozoic formation, and the whole Mesozoic section is absent in and around the area which is the sign of unconformity. The Sakesar limestone and Chorgali Formations of Eocene age are the primary reservoir of this while Permian and Cambrian sandstones are secondary targets. The Eocene, Paleocene and Permian shale are supposed to be the potential source of oil and gas.

In the area rocks from PRE-CAMBRIAN to QUATERNARY age is present in the Potwar basin. There are numerous unconformities present represent the extensive periods of uplift and erosion. The oldest rock penetrated in Fimkassar field, is the Salt Range Formation, encountered at 3633 m in the well Turkwal deep -01.

The stratigraphic column is divided into three unconformity bounded sequences. These unconformities in the study area are Ordovician to Carboniferous, Mesozoic to Late Permian, and Oligocene in age shown in Figure 2.3. These unconformities are not easily identified in the seismic profiles due to complex thrusting. The Potwar basin is filled with thick infra Cambrian evaporite deposits overlain by relatively thin Cambrian to Eocene age platform deposits followed by thick Miocene Pliocene molasse deposits. This whole section has been severely deformed by intense tectonic activity during the Himalayan Orogeny in Pliocene to middle Pleistocene time. (Aamir and Siddiqui, 2006).

The oldest formation penetrated in this area is the Infra Cambrian Salt Range formation, which is dominantly composed of halite with subordinate marl, dolomite, and shale. The Salt Range formation is best developed in the eastern salt range. The salt lies unconformably on the Precambrian basement. The overlying platform sequence consists of Cambrian to Eocene shallow water sediments with major unconformities at the base of Permian and Paleocene. The Potwar basin was uplifted during Ordovician to Carboniferous, therefore no sediments of this time interval were deposited in the basin (Aamir and Siddiqui, 2006).

The second abrupt change to the sedimentary regime is represented by the complete absence of the Mesozoic sedimentary succession, including late Permian to Cretaceous, throughout the eastern Potwar area. In Mesozoic time the depocenter was located in central Potwar, where a thick Mesozoic sedimentary section is present (Aamir and Siddiqui, 2006). The mollase deposits present in the area are Chinji, Nagri, Kamliyal, Murree and Dhokpathan formations. The major unconformity is also present between platform sequence and overlying mollase section where entire Oligocene sedimentary record is missing (Aamir and Siddiqui, 2006).

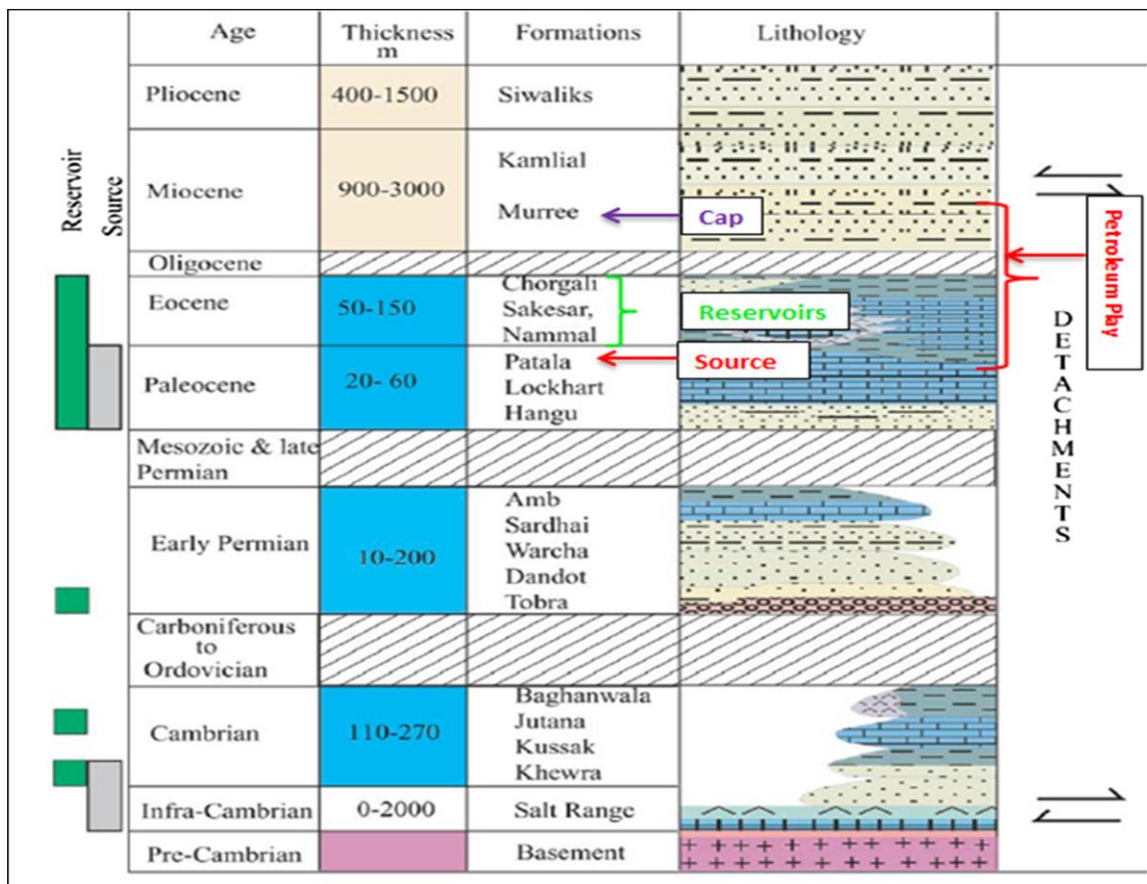


Figure 2.2 Stratigraphic Column of Eastern Potwar (Ali et al., 2014).

Petroleum Play of the Study Area

Potwar marine facies has great potential of hydrocarbon. Previous drilling was restricted up to Eocene carbonate. Recent discoveries in Potwar basin result in delineation of deep subsurface crest (Kadri, 1995).

Reservoir Rocks of Study Area

Although the effective reservoir at Fimkassar oil field lies within the Sakesar and Chorgali formations, the Nammal and Kuldana formations are also worth mentioning in this area because these four formations (Nammal, Sakesar, Chorgali and Kuldana) are part of the same depositional sequence (Vail *et al.*, 1977). The Nammal, Sakesar, Chorgali and Kuldana Sequence were deposited on a ramp which fits the classic models for Tertiary low latitude carbonate ramps (Buxton and Pedley, 1989). These are characterized by slope gradients of less than degree and extend 10 to 100 of kilometers along strike (Buxton and Pedley, 1989). Hence Paleozoic-Tertiary dominantly marine sedimentary rocks form petroleum systems in Potwar basin and are exposed in Salt Range along the frontal thrust and the fractured carbonates of Sakesar and Chorgali formations are the major producing reservoirs in the study area.

Sakesar is major formation, acting as reservoir producing both Oil and Gas in Fimkassar area. It is a fractured reservoir, having negligible porosity (matrix). It is about 70 to 300 m thick and is early to middle Eocene in age (Bender and Raza, 1995). It is named after Sakesar town in the Salt Range where it is well exposed. The Limestone present is of grey color and show stylolite. As porosity in the Sakesar formation is very low, fractures provide only form of permeability. The production from Sakesar commenced in 1980, and this formation is encountered in all the wells, used in research.

Nammal is about 34m to 130 m thick and it is of early Eocene age (Bender and Raza, 1995). It is named after the nammal gorge present in the western salt range. In the lower section of the formation shale is present where as in the upper section Limestone is present dominantly.

Chorgali formation consists of massive dolostones, marls, nodular, extremely fissile varicolored shale, chicken wire anhydrites and evaporite collapse breccia. The Chorgali formation is named following Chorgali Pass that transects the Khair-e-Murat ridge near the village, Pind Fateh. It is 80 to 90 m thick (Jurgan and Abbas, 1991) and is early middle Eocene in age .It has very slightly primary porosity but dolomitization has produce porosities up to 25%.

Figure 2.3 depicts the reservoir rocks.

Source Rocks of Study Area

The organic rich shale of the Paleocene (Patala formation) can be considered as the main formation which is acting as source to the Potwar basin (Bender and Raza, 1995). Also, Salt Range formation (Pre-Cambrian) contains oil shale intervals, which shows source rock potential. Figure 2.3 shows source rocks of the study area.

Cap/Seal Rocks of Study Area

In study area associated structures are pop up anticlines and snaked head structures. The Formation which act as a reservoir rock in the study area is Murree Formation. The clays and shales of the Murree formation also provide efficient vertical and lateral seal to Eocene reservoirs wherever it is in contact. Murree formation is highlighted in Figure 2.2.

Chapter 3

Seismic Data Interpretation and Seismic Attributes

INTRODUCTION

The Seismic data interpretation is the method of determining information about the subsurface of earth from seismic data. It may determine general information about an area, locate prospects for drilling exploratory wells or guide development of an already discovered field (Coffeen, 1986). According to Badley (1985), such reflections and unconformities are to be mapped on seismic section, which fully describe the geology and hydrocarbon potential of the area. If the horizon of interest is not prominent and it is difficult in tracing it over the whole area, it is advisable to pick additional horizons above and/or below the target horizon. This helps in understanding the trend and behavior of the target horizon in the zones where its quality is not good enough to be picked with confidence. Final objective of interpretation is conversion of seismic section into a geological section which provides a somewhat realistic subsurface picture of that area, both structurally as well as stratigraphically (Badley, 1985).

We transform the whole seismic information into structural or stratigraphic model of the earth with the help of interpretation. As the seismic section is the representative of the geological model of the earth, by interpretation, we try to locate the zone of final anomaly. Not only a good interpretation be consistent with all the seismic data, it also important to know all about the area, including gravity and magnetic data, well information, surface geology as well as geologic and physical concept (Sheriff, 1999).

An interpreter of seismic data may have good hold in both geology and geophysics. It is the ingenuity and in-depth understanding of an interpreter to extract geologic significance from aggregate of many minor observations. For example, down dip thinning of the reflection might be result from normal increase velocity with depth or thinning of the sediments or flow of the shale or salt may develop illusory structure in the deeper horizon (Sheriff, 1999).

Interpretation is the transformation of seismic reflected data into a structural picture by the application of corrections, migration and time depth conversion. Seismic reflection method uses

sound waves to investigate the subsurface. The acoustic impedance governs the reflection, which is one of the rock properties (Dobrin and Savit (1988)).

There are two main approaches for the interpretations of a seismic section are:

- Stratigraphic Analysis
- Structural Analysis

Stratigraphic Analysis

An analysis of the history, composition, relative ages and distribution of strata, and the interpretation of strata to elucidate Earth history. Stratigraphy analysis involves the delineating the seismic sequences, which present the different depositional units, recognizing the seismic facies characteristic with suggest depositional environment and analysis the reflection characteristic variation to locate the both stratigraphy change and hydrocarbon depositional environment . The amplitude, velocity, frequency or the change in wave shape indicates hydrocarbon accumulation. Unconformities are marked by drainage pattern that help to develop the depositional environment. Reef, lenses, unconformity are example of stratigraphy traps (Sheriff, 1999).

Structural Analysis

In structural analysis we find out the structural traps in which tectonics play an important role. Tectonics usually tell us which type of structures are present and how they can be related with each other so tectonic of the area is helpful in determining the structural style of the area and to locate the traps. Structural traps include the faults, folds anticline, pop up, duplex, etc. (Sheriff, 1999). A fault with throw less than $\frac{1}{4}$ of the wavelength of seismic wave will difficult to pick in the seismic section (Badley, 1985). The study area lies in intense compressional regime, so general structure are thrusts related i.e. pop up structure. A thrust fault develops under high pressure system and to develop, it required high pressure under the thrust plane.

A workflow of structural analysis is shown in Figure 3.1.

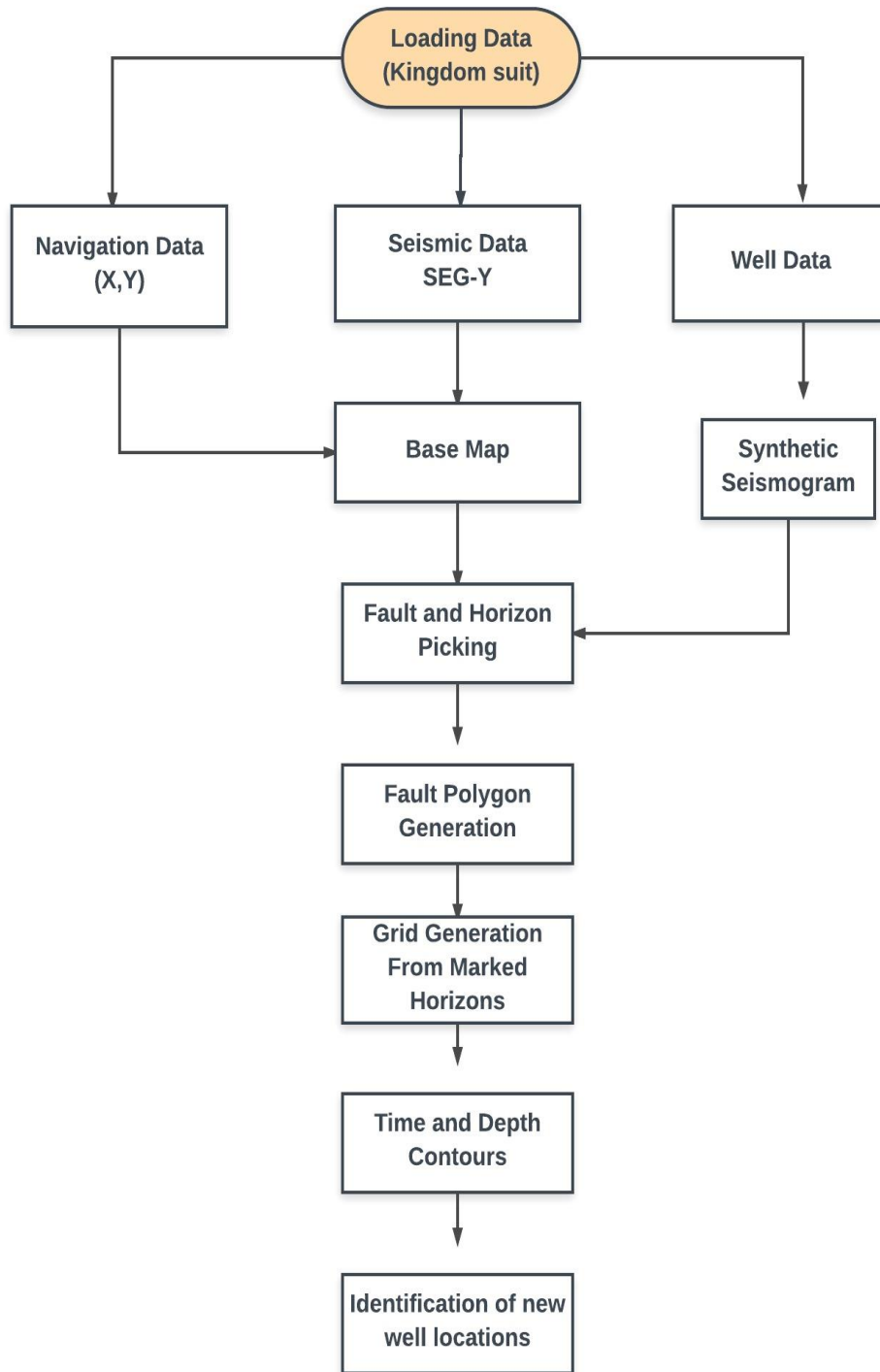
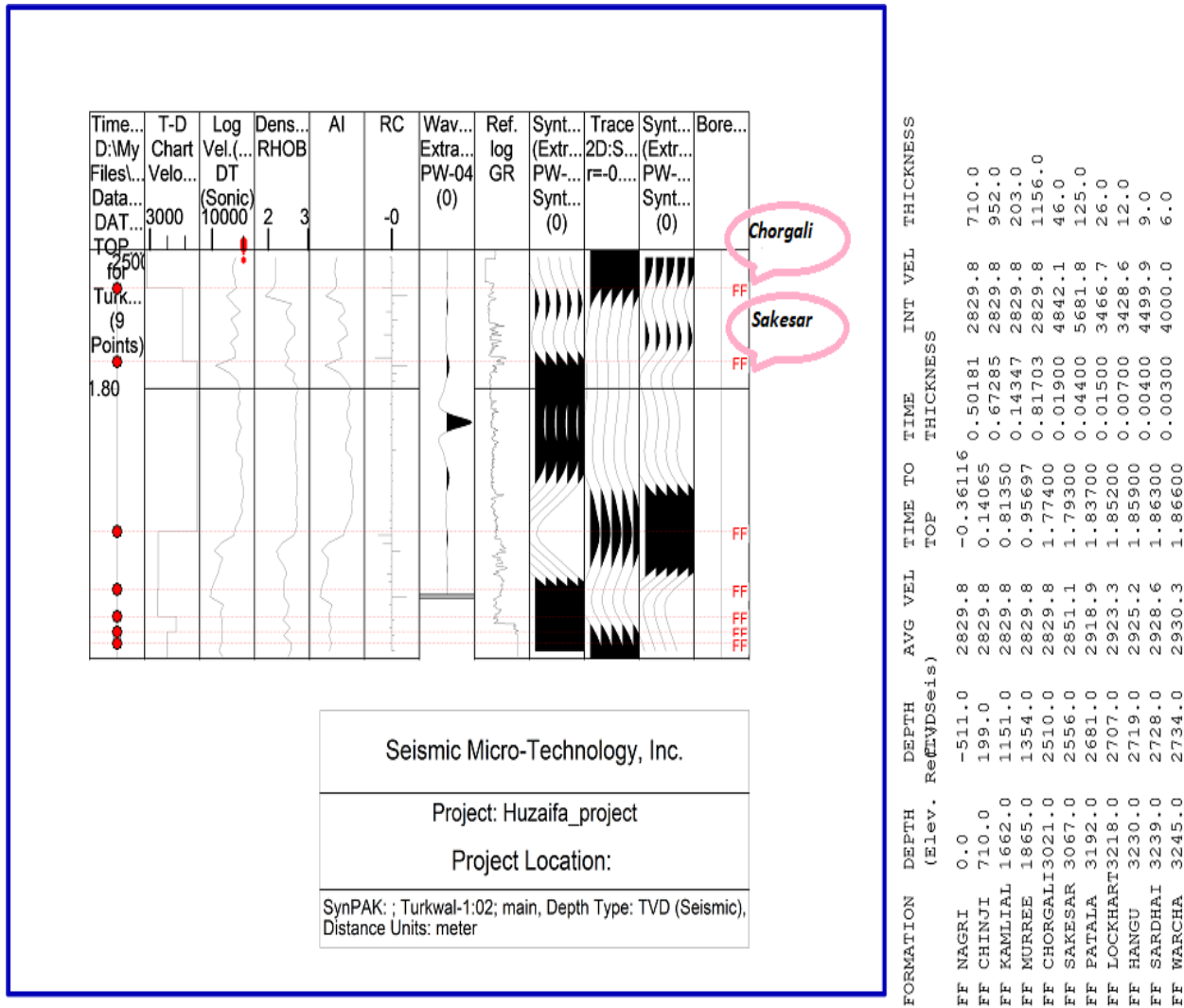


Figure 3.1 Workflow

Synthetic Seismogram

The synthetic seismogram is generated by convolving the reflectivity derived from digitized acoustic and density logs with the wavelet derived from seismic data. By comparing marker beds or other correlation points picked on well logs with major reflections on the seismic section, interpretations of the data can be improved. The quality of the match between a synthetic seismogram depends on well log quality, seismic data processing quality, and the ability to extract a representative wavelet from seismic data, among other factors. The acoustic log is generally calibrated with check-shot or vertical seismic profile (VSP) first-arrival information before combining with the density log to produce acoustic impedance. Figure 3.2 shows the picture of synthetic seismogram.



Huzaifa Athar@HUZAIFAATHAR
07/12/17 00:31:17

Figure 3.2 Synthetic Seismogram.

Interpretation of Seismic lines

The interpretation of seismic lines includes following steps.

- Identification of faults.
- Marking of seismic horizons.

Identification of Faults

Three faults are marked on the seismic sections indicates the complexity of the study area. These are marked on observing the sudden change in the position of the reflectors and distortion or disappearance of the reflection below the faults. All the faults are not basement rooted that gives some indication of thin skin tectonic involvement in the study area but the normal faulting is present in basement. Faults marked are shown in Figure 3.3 and 3.4. In Figure 3.3 line PW-04 is marked and in Figure 3.4 line PW-06 is marked.

Marking of Seismic Horizons

Primary task of interpretation is the identification of various horizons as an interface between geological formations. For this purpose, good structural as well as stratigraphic knowledge of the area is required. Thus during interpretation process, both the horizons and faults are marked on the seismic sections (McQuillin, *et al.* 1984). Chorgali, Sakesar and Patala formations are marked. The marked horizons are shown in Figure 3.3 and 3.4.

Interpreted Seismic Sections

Two Dip line namely PW-04 and PW-06 are interpreted. Three faults are marked on each line. Three horizons namely Chorgali, Sakesar of Eocene and Patala of Paleocene age are marked. These horizons and faults are identified on seismic section in Figure 3.3 and 3.4.

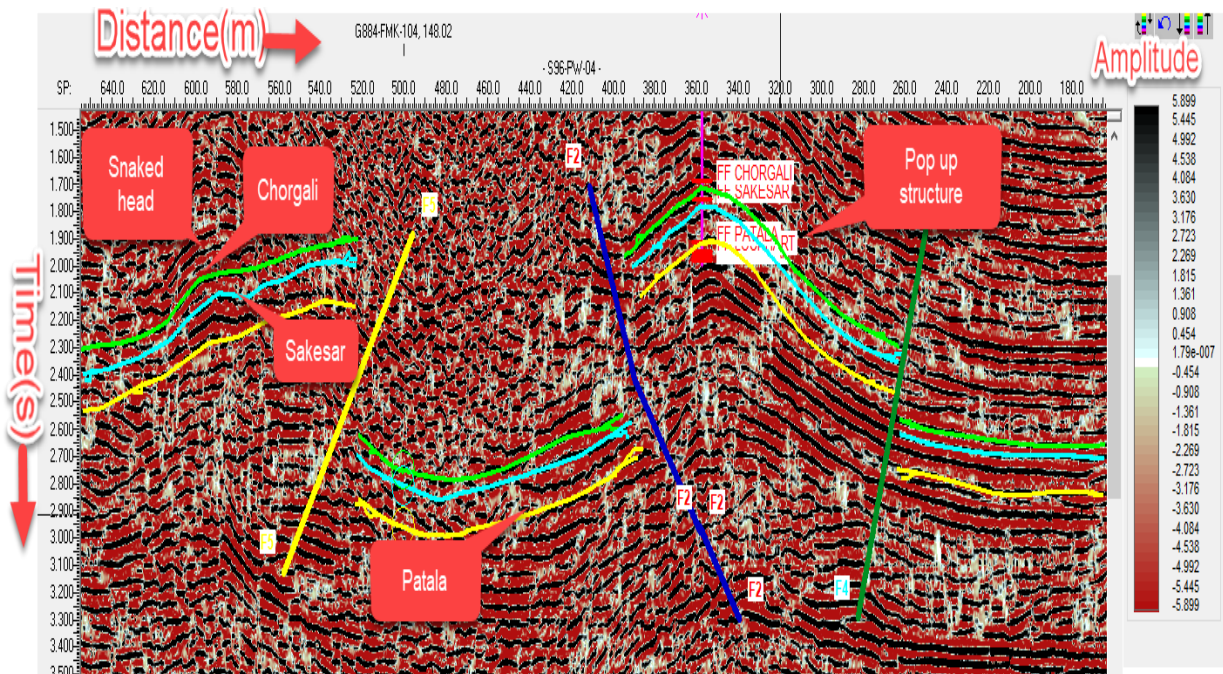


Figure 3.3 Seismic Section of Line PW-04.

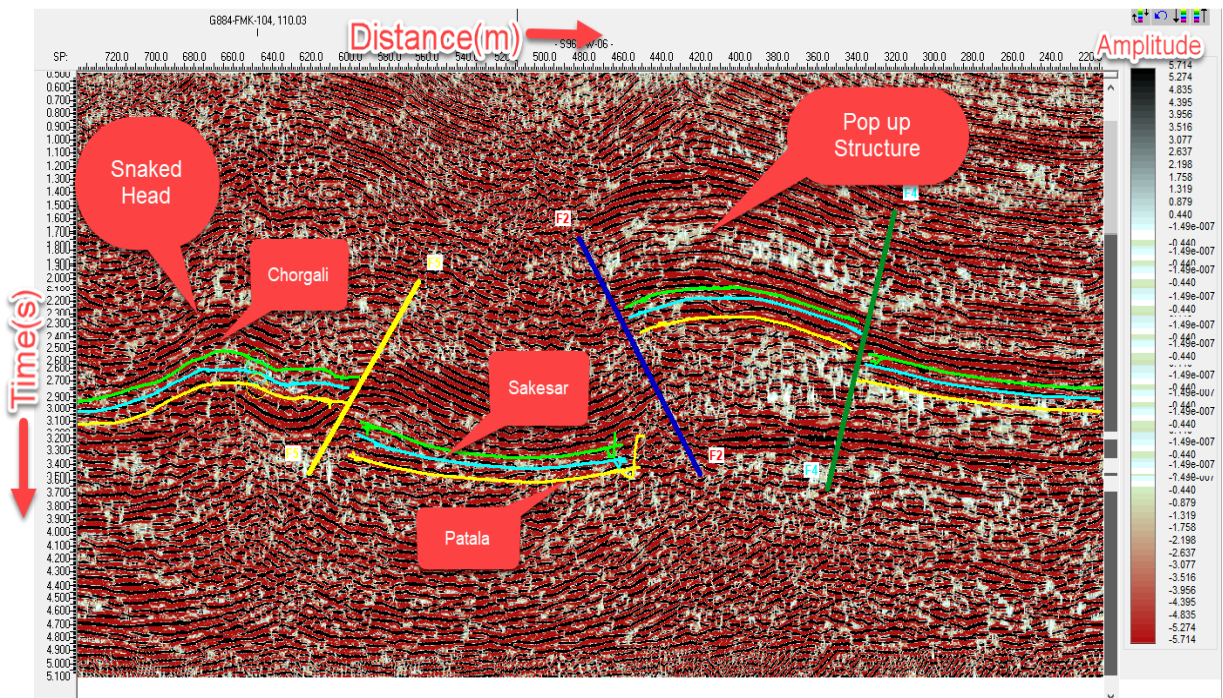
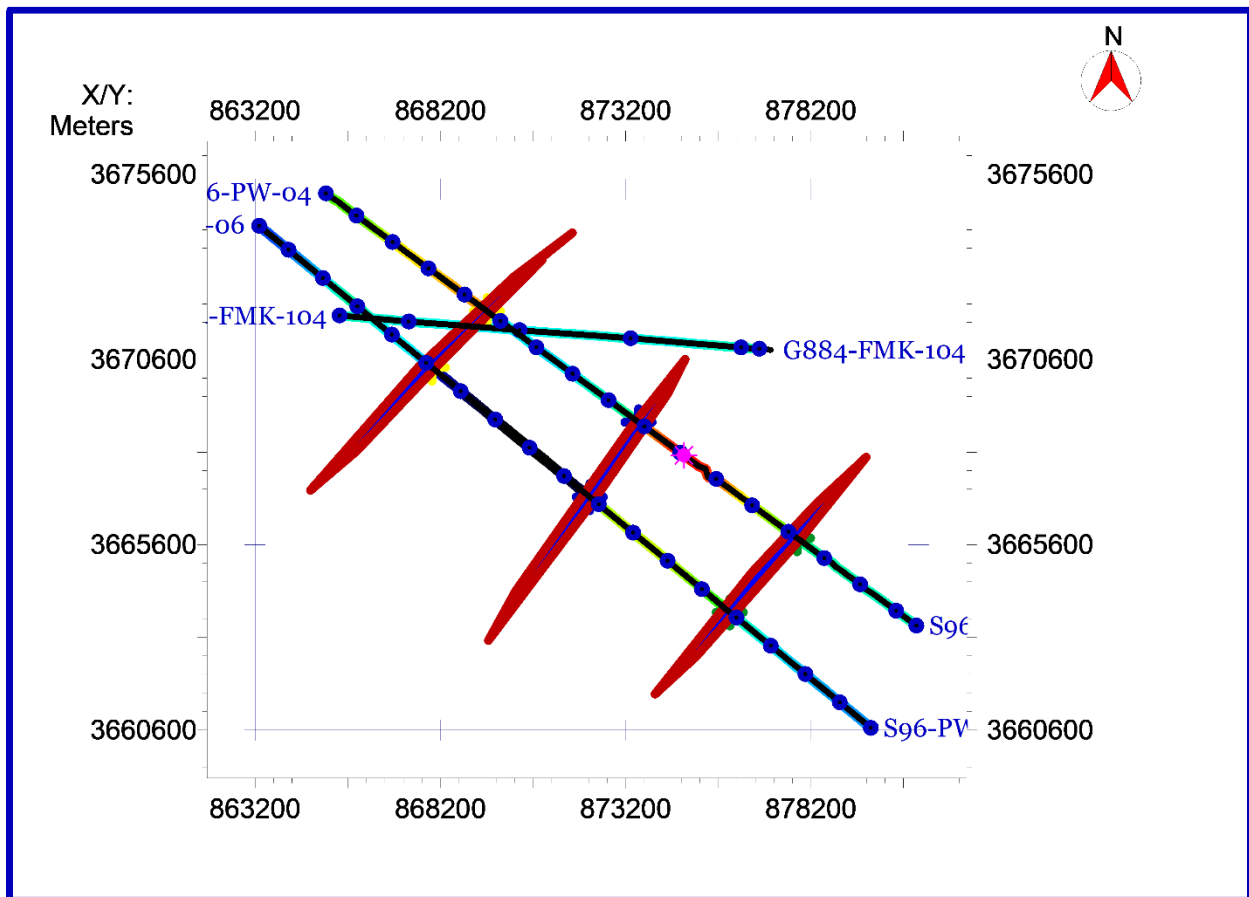


Figure 3.4 Seismic Section of Line PW-06.

Fault Polygons Generation

A fault polygon represents the lateral extent of dip faults having same trend. Fault polygon show the sub-surface discontinuities. To generate fault polygon, it is necessary to identify the faults and their lateral extent if one finds that the same fault is present on all the dip lines, then all points (represented by “x” sign by Kingdom software) can be manually joined to make a polygon. Construction of fault polygons are very important as far as two-way time and depth contouring of a horizon is concerned. The reason that if fault is not converted into polygon the software doesn't recognize it as a barrier or discontinuities, thus represent a false picture of the subsurface. After construction of fault polygons, the high and low areas on a particular horizon become obvious. Fault polygons are constructed for all marked horizons and these are oriented in NE-SW direction. The fault polygon is shown in Figure 3.5.



Huzaifa Athar@HUZAIFAATHAR

Figure 3.5 Fault Polygons

Contour Maps

Mapping is part of the interpretation of the data. Contour maps are constructed on basis of seismic interpretation. The contours are the lines of equal time or depth wandering around the map as dictated by the data (Coffeen, 1986). In constructing a subsurface map from seismic data, a reference datum must be selected first. The datum may be sea level or any other depth above or below sea level. Contouring represents the 3D earth on a 2D surface. The spacing of the contour lines is a measure of the steepness of the slope i.e. closer the spacing, steeper the slope.

Time and Depth Contour Maps of Chorgali Formation

The time and depth map of Chorgali Formation are generated on the base map along with wells and their corresponding fault polygons shown in Figure 3.5. The polygon F2, F4, F5 shows dipping in NE-SW direction. The time contour map of Chorgali Formation is shown in Figure 3.6. The contour interval for time contours is set as 50msec and that of depth contour is 80m. The structural variation in these contours can be interpreted by using color bar and legends.

The depth contour map of Chorgali Formation was calculated from the time contour map by using velocity obtained from DT-log run in Chorgali Formation using formula

$$s = \frac{vt}{2}. \quad (3.1)$$

Where,

s = Distance

v = Velocity

t = Time

The depth variation in contour map is interpreted by using color bar shown in Figure 3.7.

Kingdom has the built-in function of showing negative values for depth below mean sea level.

This mean sea level is the reference point.

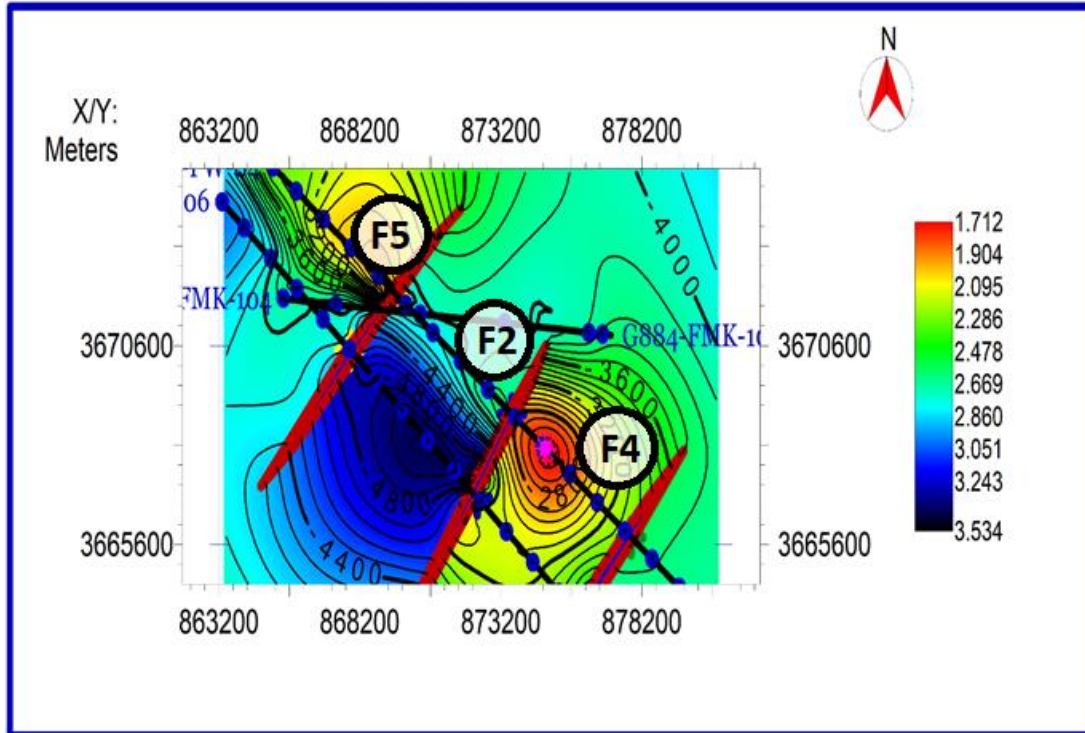
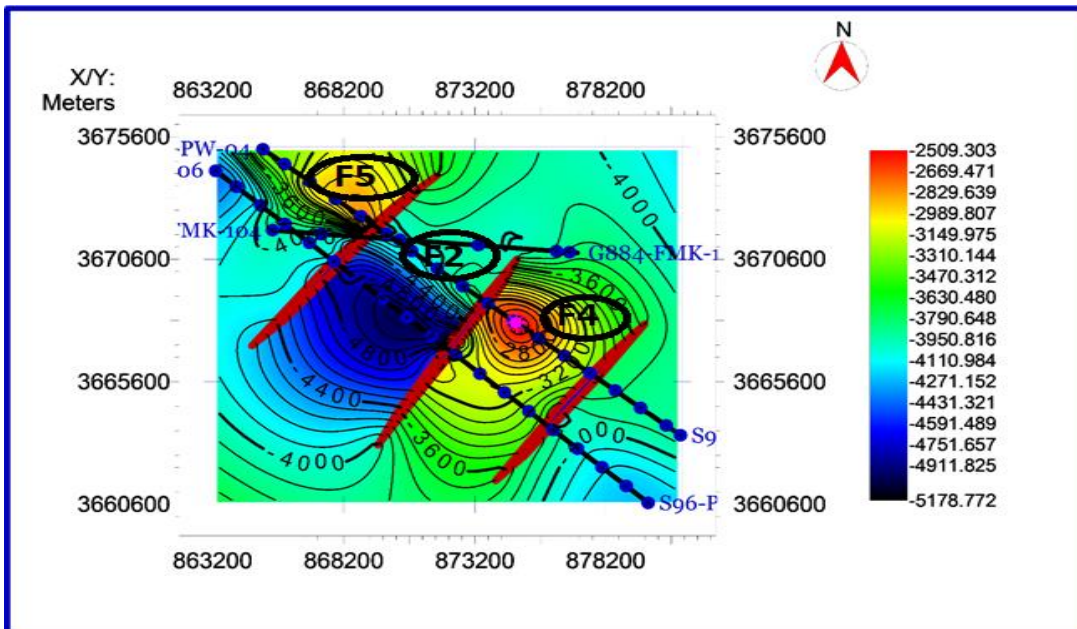


Figure 3.6 Time contour map of chorgali formation.

The orange color ranges from (1.904s-2.095s) shows the shallowest part and blue color approaches from (3.051s-3.243s) shows the deepest part.



Huzaiifa Athar@HUZAIFAATHAR

Figure 3.7 Depth Contour map of chorgali formation.

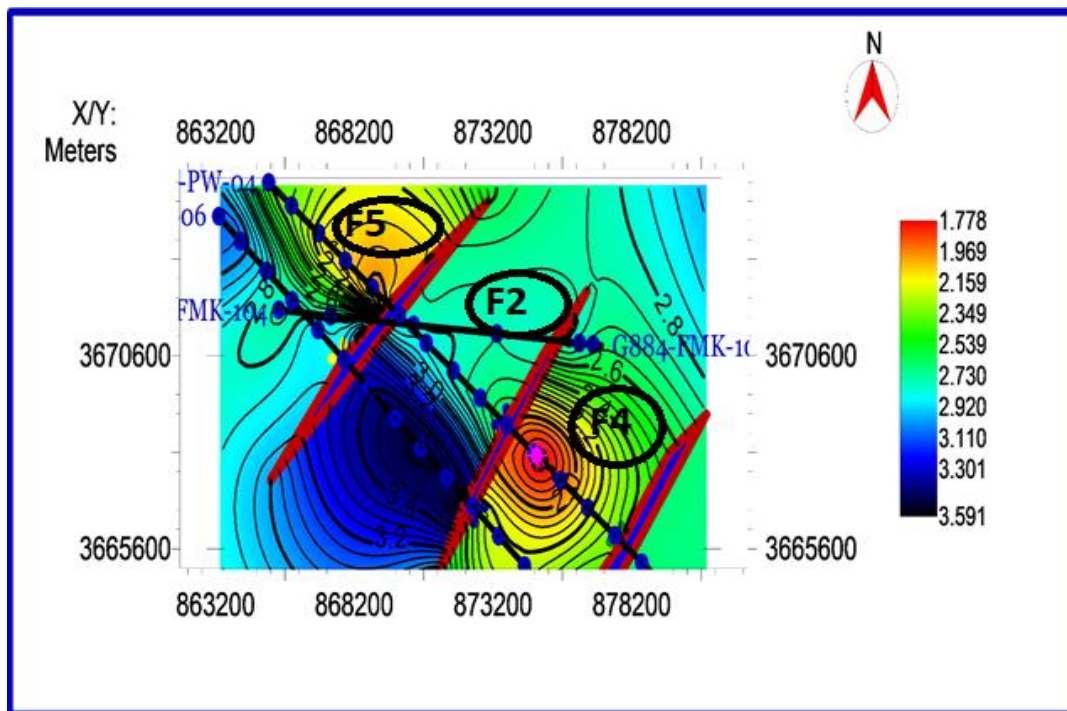
The orange color from (2669m-2829m) shows the shallowest part while blue color from (4751m-4911m) shows the deepest part.

Following interpretations are made from these time and depth contours shown in the Figures 3.6 and 3.7 given below

- The interpreted structure for Chorgali Formation is a pop-up anticline and snaked head structure.
- The pop up anticline is bounded by thrust faults F2 and F4 and snaked head structure is formed due to thrust fault F5.

Time and Depth Contour Maps of Sakesar Formation

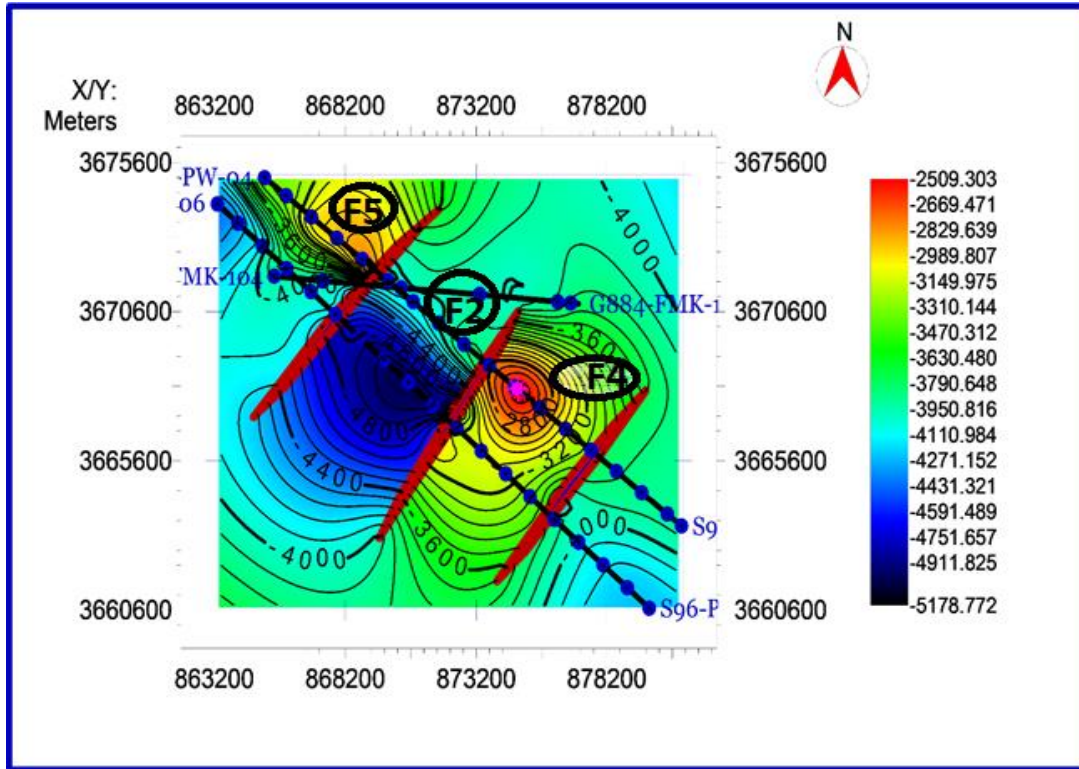
The time contour map of Sakesar Formation is shown in Figure 3.8. The contour interval for time contours is set as 50ms and that of depth contour is 80m. The structural variation in these contours can be interpreted by using color bar and legends. The orange color ranges from (1.969s-2.159s) shows the shallowest part and blue color ranges from (3.110s-3.301s) shows the deepest part.



Huzaifa Athar@HUZAIFAATHAR

Figure 3.8 Time contour map of Sakesar formation.

The depth variation in contour map is interpreted by using color bar shown in Figure 3.9. The light blue color from (2542m-2750m) shows the shallowest part while orange color from (4724m- 5140m) shows the deepest part.



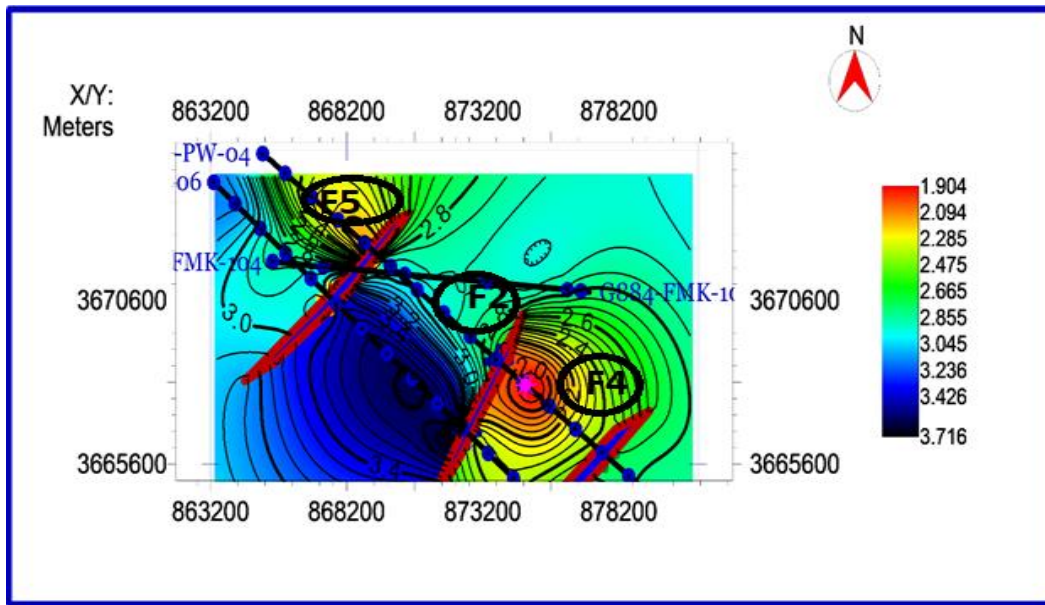
Huzaiifa Athar@HUZAIFAATHAR

Figure 3.9 Depth Contour of Sakesar Formation.

Time and Depth Contour of Patala Formation

Time and depth contour map of Patala Formation are given below in Figure 3.10 and Figure 3.11 respectively.

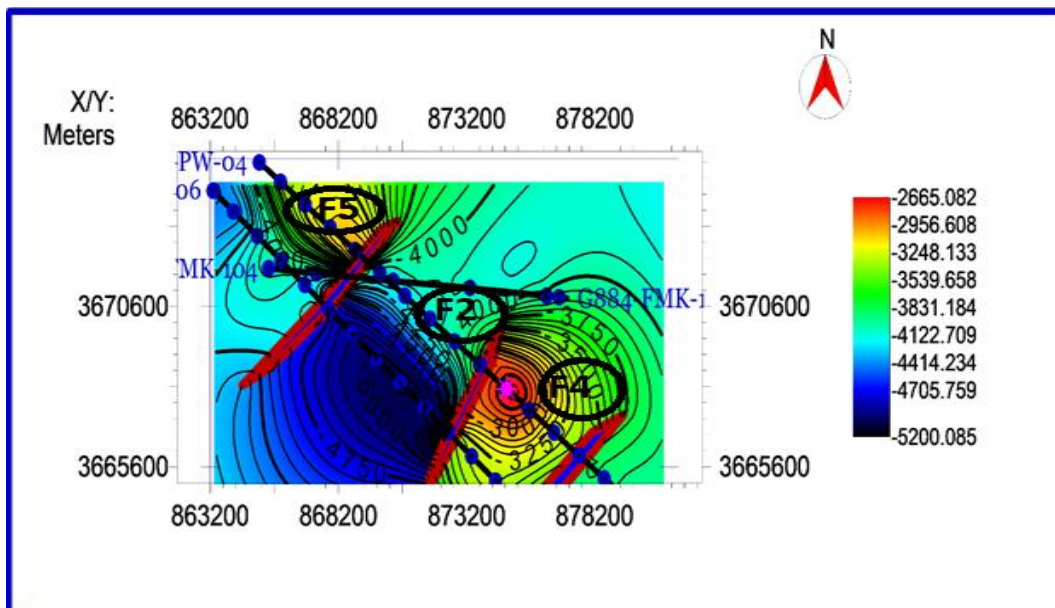
The time and depth maps can be interpreted by using same techniques as we have done in previous Formations. The contour map shown in Figure 3.10 almost gives same structure interpretation as of previous two Formations discussed above. The TWT contour map can be interpreted from the color bar. The orange color ranges from (2.094s-2.285s) shows the shallowest part or elevated part is our zone of interest. It is interpreted as pop-up structure because value of time is decreasing as we move outward. The deepest part is shown by blue color ranging from time values 3.236s to 3.426s.



Huzaifa Athar@HUZAIFAATHAR

Figure 3.10 Time Contour Map of Patala Formation.

The depth map of Patala Formation can also be interpreted by using a color bar. Figure 3.11 shows the depth map of Patala Formation. The depth value ranges from (2665.082m-2956.608m) shown by orange color and depth values ranges from (4414.234m-4705.759m) represents the deeper part which are shown by blue color.



Huzaifa Athar@HUZAIFAATHAR

Figure 3.11 Depth Map of Patala Formation.

Identification of Well Location

The purpose of generating contour map is to find to determine the area where hydrocarbons accumulate. The hydrocarbon mostly accumulates in the regions of low pressure and permeability. Ideally these regions are hinge of the anticlines. In real case the hinge of anticline are also structurally disturbed and there is a risk of drilling in that location (Coffeen, J.A., 1986).

The lead is a three-way dip structure comprised of snaked head structure shown in Figure. Two side of closure is controlled by thrust fault and third side is controlled by dip of the structure. This lead represents time (1.929s) at Chorgali in Figure 3.12, Sakesar at (1.985s) in Figure 3.13 and Patala Formation at time (2.150s) in Figure 3.14.

The lead here is marked on the basis of the low amplitude. This low amplitude is shown by yellow color and this color shows low amplitude. As this lead is near fault and is on the line so the entrapment is possible here.

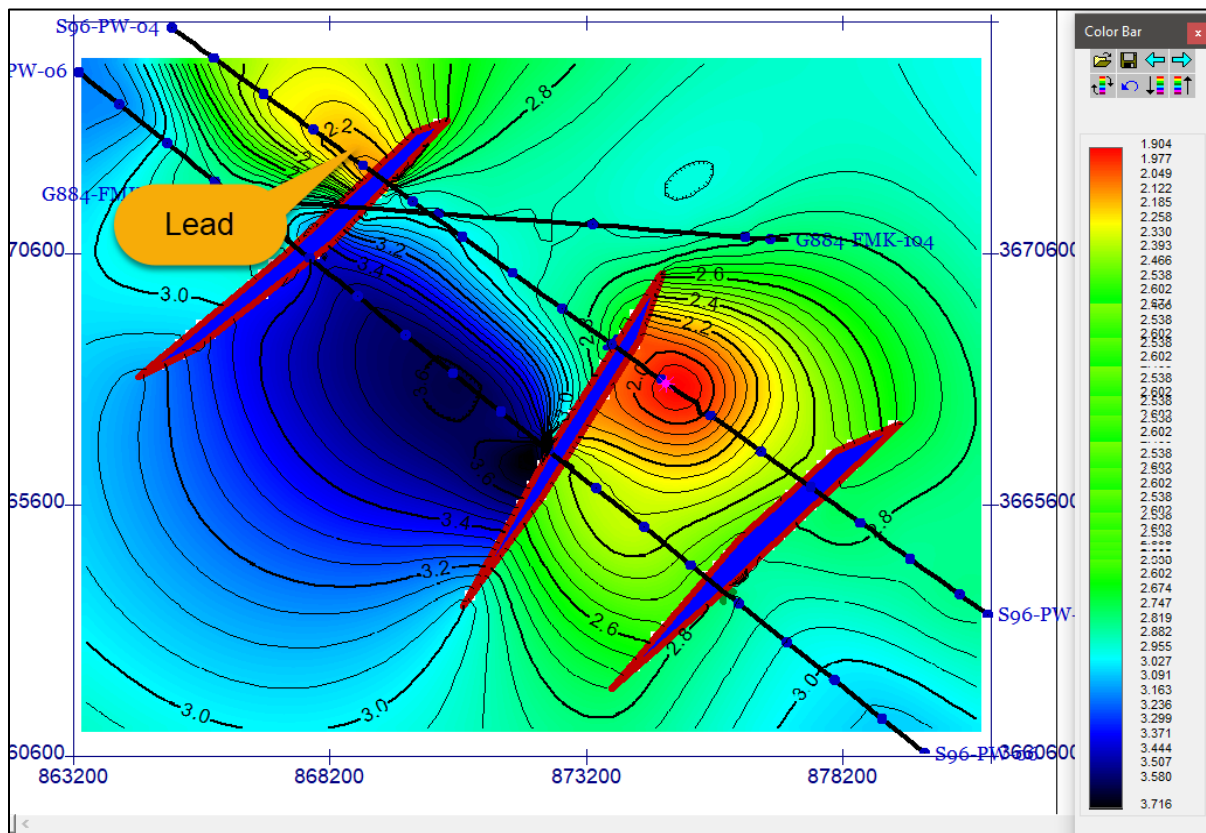


Figure 3.12 Lead shown in Chorgali Formation.

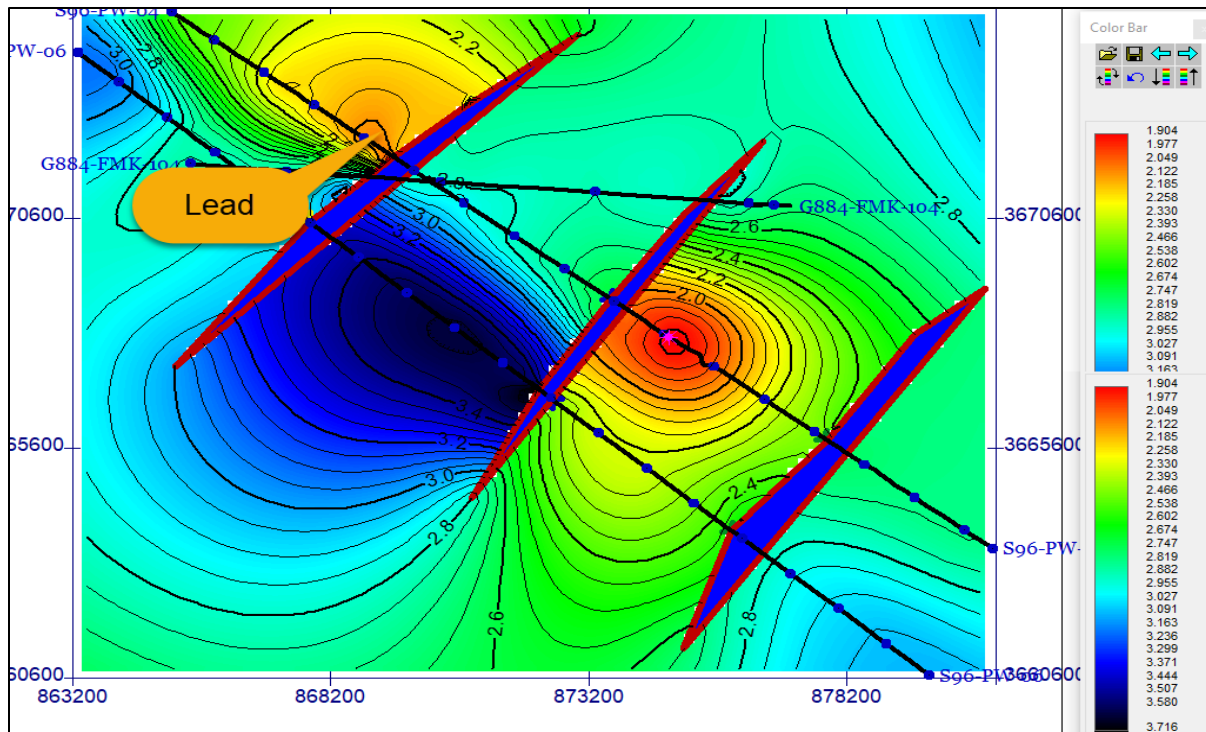


Figure 3.13 Lead shown in Sakesar Formation.

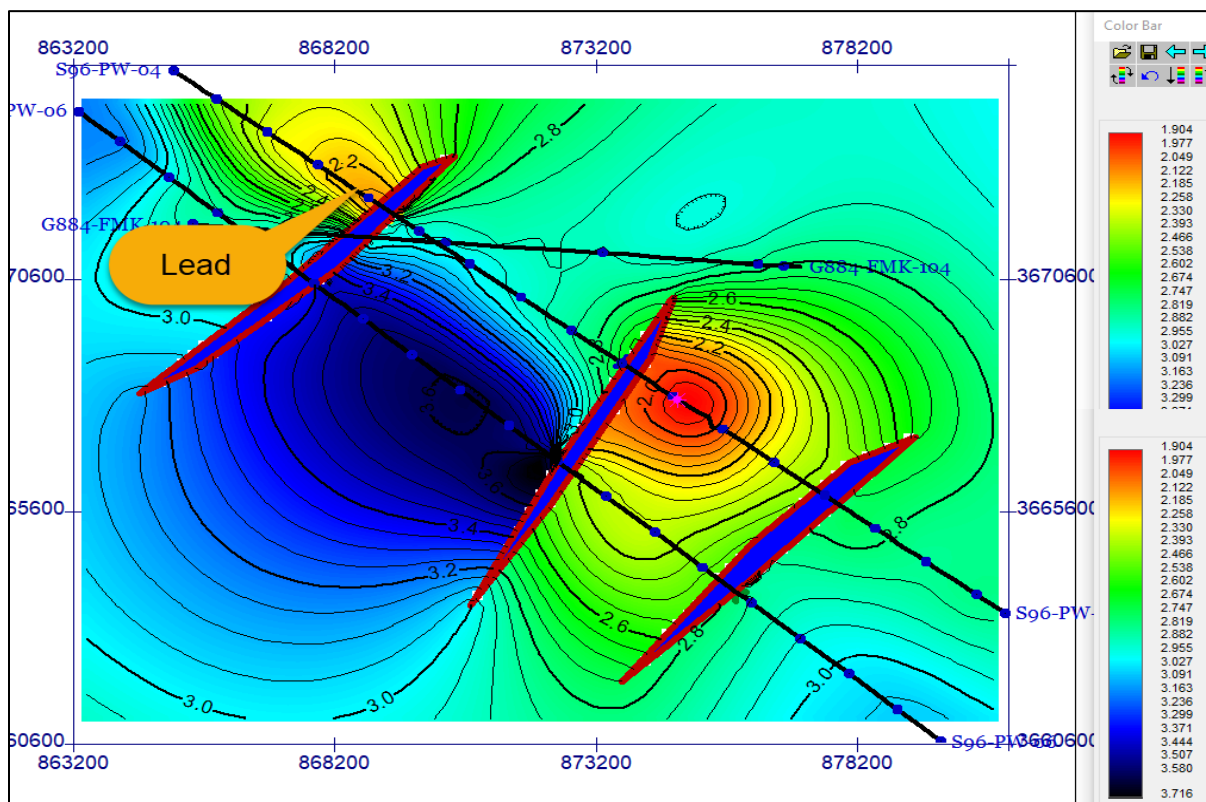


Figure 3.14 Lead shown in Patala Formation.

Seismic Attributes

Attributes are the built in properties of seismic wave signal which are acquired from seismic data. Seismic waveform carry important subsurface geological information so the extraction of attributes can be useful to retrieve this information (Nanda, 2016). The default attribute of seismic data in Amplitude.

These attributes have two categories.

- Primary Attributes
- Geometric Attributes

Primary Attributes

These attributes are based on seismic amplitude and are extensively used to predict the rock-fluid parameters, which in some conditions, serve as direct hydrocarbon indicators. The variation in amplitude along a horizon gives us information about lithology and porosity of that area (Nanda, 2016). Some of the primary attributes include

- Instantaneous Frequency
- Instantaneous Phase
- Trace envelope

Geometric Attributes

These attributes define the geomorphology of subsurface structural and stratigraphic features including their lateral variations. These attributes are very helpful in reliable interpretation of subsurface features especially in reservoir characterization (Nanda, 2016).

Reflection Strength or Trace Envelope

It is the amplitude of envelope of an event. Independent of phase which means the reflection strength maxima may be different from the maximum amplitude seen at peak or trough of reflection. Sharp lateral variation is indicative of major lithological change, faults, unconformities and gas saturation. Gradual changes may be linked to lateral changes in lithofacies and bed thickness (Nanda, 2016).

This attribute is computed for seismic line PW-04 shown in Figure 3.15, to see the major changes in lithologies. Even negative reflection coefficients such as limestone formation overlaid

on clayey formation would generate a positive response in this attribute. This positive response is because limestone is a compact lithology and has high density.

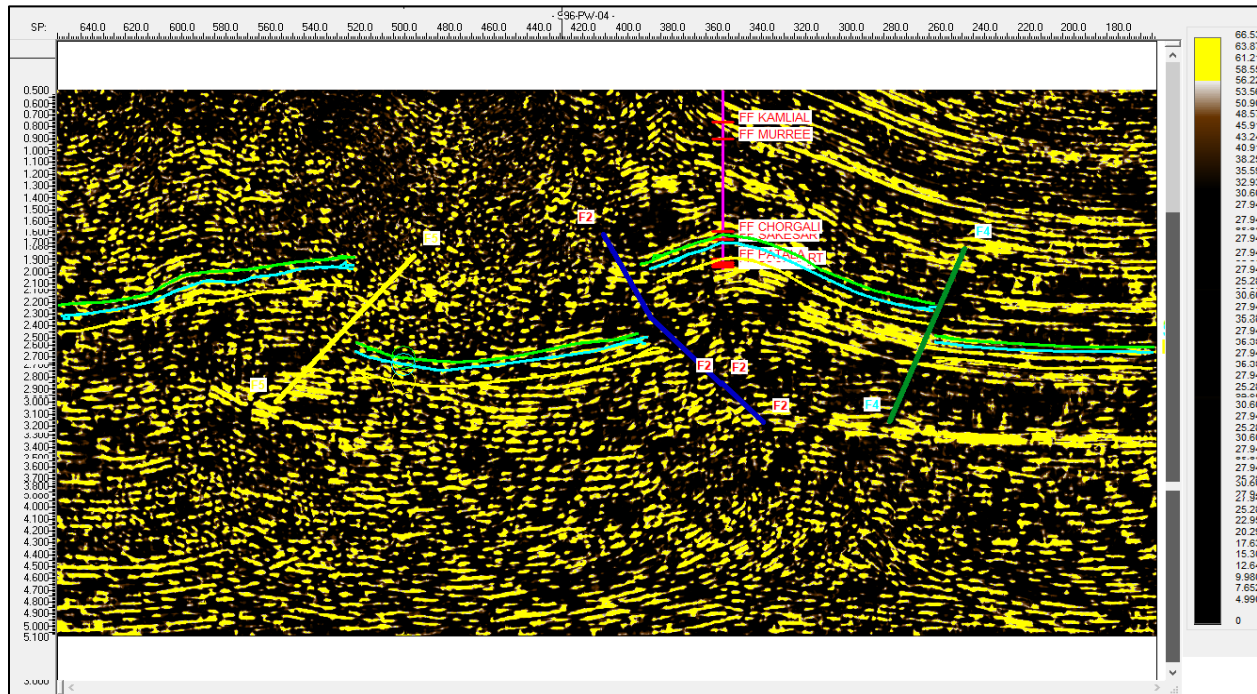


Figure 3.15 Reflection strength attribute.

When the envelope attribute is applied there is a thick package of yellow color is shown which indicates the strong reflection strength from our reservoir rocks. This also shows that there is a variation in the thickness of limestone and a breakage present indicates the fault. This also confirms that we mark the horizons at the true location.

Instantaneous Phase

This section displays the phase of a reflection waveform at a time corresponding to peak, trough and zero crossing. It is independent of amplitude and does not vary with strong or weak reflection events. Phase correlation can be extremely useful in tracking continuity of reservoir facies where amplitude correlation does not help due to impedance contrast. It emphasizes lateral discontinuities of features like faults and pinch outs better (Nanda, 2016). Figure 3.16 shows the attribute of instantaneous phase on seismic section of line PW-06.

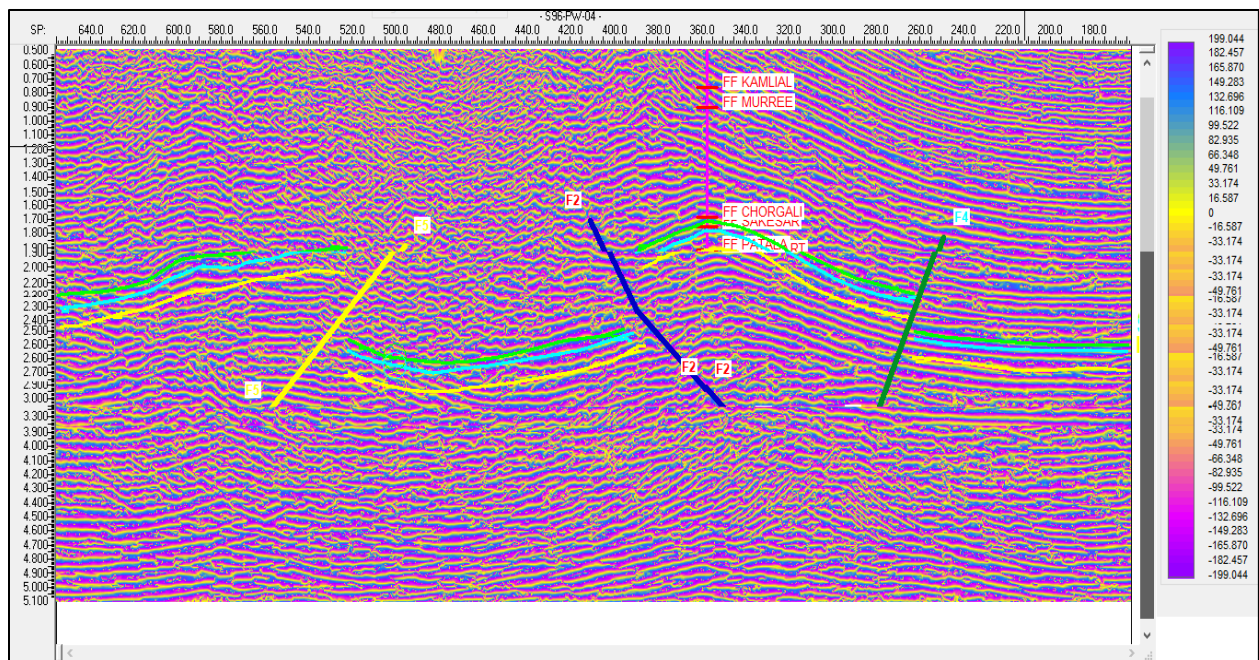


Figure 3.16 Instantaneous Phase.

Figure 3.16 shows the instantaneous phase attribute which changes from 199.044 to -199.04. This instantaneous phase is measured in degrees. The interpreted horizons lie over the zero phase regions indicated by yellow color. This attribute further confirms the interpretation as the input data is zero phase. It can be observed in comparison to amplitude-based sections that the instantaneous phase shows much deeper horizons.

Chapter 4

Petrophysical Analysis

Introduction

The physical properties of rocks such as volume of shale, porosity, water and Hydrocarbon saturation which are used for identifying hydrocarbon zones are obtained by Petrophysics using wireline logs, core and production data (Ali et al., 2014). It provides a means to evaluate the hydrocarbon potential zones in a reservoir (Ellis and Singer, 2007). Petrophysics uses the data of well logs, core and production data to predict the physical properties of rocks such as porosity, volume of shale, water saturation to identify the hydrocarbon bearing zones (Ali et al., 2014).

Data Used

Data for the well Fimkassar-02 was used for Petrophysical analysis to estimate the probable zones of Hydrocarbon.

Logs Used

The logs used, in Petrophysical analysis, which are run in Fimkassar-02 are shown in Table 4.1.

Table 4.1 Logs Used and their Scales

	<i>Type of Logs</i>	<i>Acronym</i>	<i>Scale Used</i>	<i>Units</i>
1	Caliper Log	CALI	4.0-14.0	Feet
2	Spontaneous Log	SP	-100-100	mV
3	Gamma Ray Log	GR	0-150	API
4	Micro-Spherical Focused Log	MSFL	0.20-2000	Ω m
5	Laterolog Deep	LLD	0.20-2000	Ω m
6	Laterolog Shallow	LLS	0.20-2000	Ω m

7	Sonic Log	DT	140-40	$\mu\text{sec}/\text{ft}$
8	Neutron Log	NPHI	0.45- (-0.15)	PU
9	Density Log	RHOB	1.95-2.95	gm/cm^3

Workflow

Following workflow was followed for petrophysical interpretation.

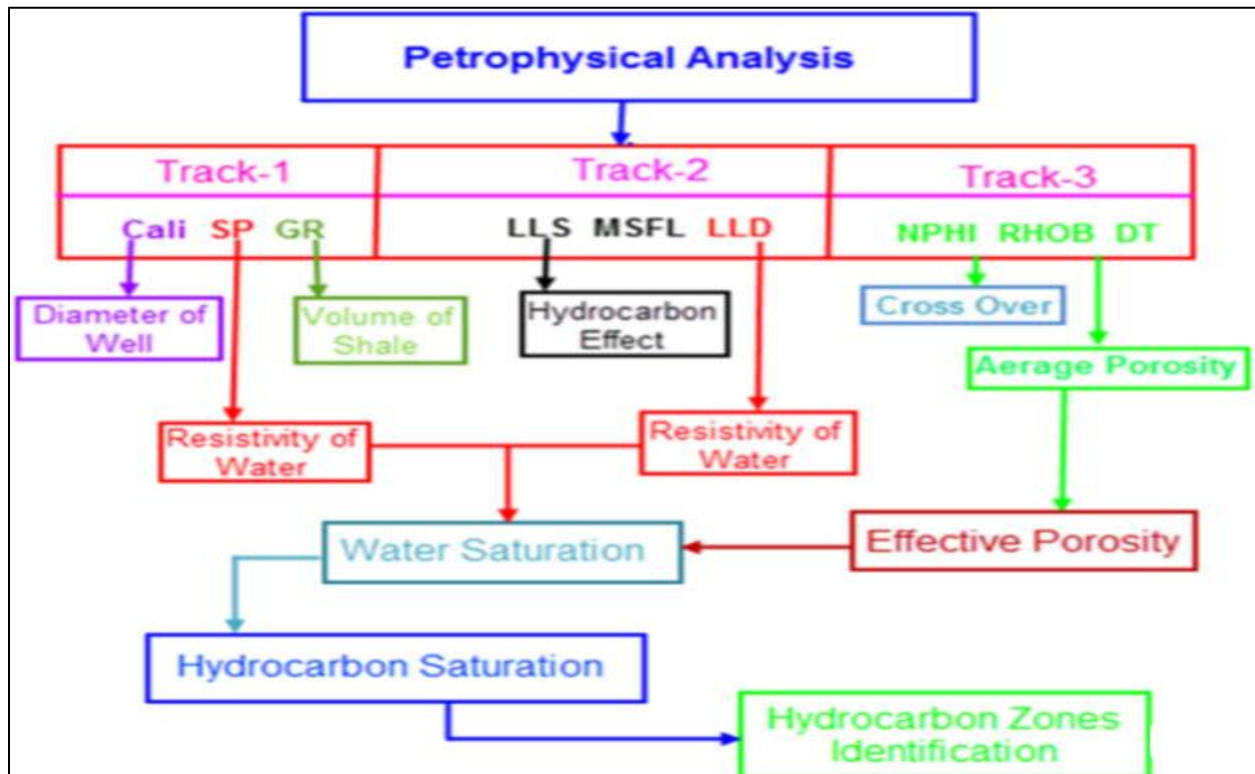


Figure 4.1 Workflow for Petrophysics (Ali et al., 2014).

Tracks

A specific arrangement of logs in Track 1, 2 and 3 is followed during the presentation of logs. In Table 4.2, this arrangement of logs is shown. The Petrophysical analysis, which I performed in my dissertation, follows this track pattern.

Table 4.3 Logs Used in different Tracks

<i>Tracks</i>	<i>Logs</i>
Track:1	<ul style="list-style-type: none">• Caliper log• SP log• GR log
Track:2	<ul style="list-style-type: none">• MSFL• LLD• LLS
Track:3	<ul style="list-style-type: none">• NPHI• RHOB• DT
Track:4	<ul style="list-style-type: none">• VSH
Track:5	<ul style="list-style-type: none">• PHID
Track:6	<ul style="list-style-type: none">• PHIT
Track:7	<ul style="list-style-type: none">• PHIE
Track:8	<ul style="list-style-type: none">• SW
Track:9	<ul style="list-style-type: none">• HC saturation

Objective

The petrophysics analysis has been carried out in order to measure the reservoir characterization of the Fimkassar area using the borehole data of Fimkassar-02 well. Log curves including spontaneous potential log (SP), Gamma ray (GR), sonic log (DT), Laterolog Deep (LLD), Laterolog Shallow (LLS), Neutron log, density log were used for petro physical analysis the following parameters are calculated for reservoir rock.

- Volume of shale
- Porosity
- Water saturation
- Hydrocarbon Stauration

Volume of Shale:

Volume of shale can be calculated from different logs like resistivity logs, SP log and gamma ray log. In this study gamma ray log is used to calculate shale volume.

Gamma Ray Log:

The gamma ray log is the passive logging because we measure the Formation properties without using any source. Actually, it is the measures the Formation radioactivity. The gamma ray emits from the Formation in the form of the electromagnetic energy which are called the photon. When photon collides with the Formation electron hence they transfer the energy to the Formation electron so the phenomenon of the Compton scattering occurs. Now these emitted Gamma rays reached to the detector of the gamma ray and counted and displayed as count per second which is termed as the Gamma ray (Asquith and Gibson, 2004).

Calculation of Volume of Shale:

The volume of the shale is calculated by using equation given below.

$$\mathbf{IGR} = \frac{GR(log) - GR(min)}{GR(max) - GR(min)}$$

Where,

IGR= Gamma ray index.

GR (max) = Maximum value of Gamma ray reading (Shale).

GR (min) = Minimum value of Gamma ray reading (Clean Sand).

GR (log) = Gamma ray reading of formation.

Porosity:

Porosity is created due to inter granular spaces, voids formed by dissolution of grains as well as fracturing of rocks. The porosity is expressed either by percentage or in decimals. The primary porosity is developed between the grains at the time of deposition, but due to fracturing and dissolution the pore spaces become void creating secondary porosity. Secondary porosity is mainly observed in limestone. In this work porosity is calculated for different zones of interest by using the following logs, sonic log, neutron log, density log.

Sonic Log:

Sonic log device consists of a transmitter that emit sound waves and a receiver that picks and record the compressional waves as it reaches the receiver. This log is a recording verses depth of

time (t) which is required by a compressional wave to go across 1 feet of formation, called interval transit time Δt , while it is the reciprocal of the velocity of sound wave. This time (Δt) is depended upon lithology and porosity of the formation (Asquith and Gibson, 2004).

Calculation of Porosity from Sonic Log:

The mathematical relation used for calculating the porosity from sonic log is given below.

$$\Phi_s = \frac{\Delta t(\log) - \Delta t(mat)}{\Delta t(fl) - \Delta t(mat)}$$

Where,

Φ_s = Sonic Porosity.

$\Delta t(\log)$ = Log response.

$\Delta t(\text{matrix})$ = Transit time in matrix.

$\Delta t(\text{fluid})$ = Transit time in fluid.

Density Log Porosity:

Gamma rays collide with electrons in formation and scattered gamma rays received at detector and counted as indicator of formation density. An increase in counting rate causes a decrease in bulk density of formation and vice versa. (Tittman and Wahal, 1965).

Calculation of Porosity from Density Log:

The mathematical relation used for calculating the porosity from sonic log is given below.

$$\Phi_D = \frac{\rho_m - \rho_b}{\rho_m - \rho_f}$$

Where,

ρ_m = Matrix density.

ρ_b = Bulk density.

ρ_f = Fluid density.

Average Porosity:

Average porosity is the sum of all the porosities calculated by different logs divided by number of logs used for calculating the porosity. The relation for calculating the average porosity is given below.

$$\Phi_{\text{avg}} = \frac{\Phi_s + \Phi_d}{2}$$

Where,

Φ_{avg} = Average porosity

Φ_s = Sonic porosity.

Φ_d = Density porosity.

Total Porosity:

The help of following formula has calculated total porosity

$$\Phi_T = 2(\Phi_s + \Phi_d)$$

Where,

Φ_T = Total porosity.

Φ_s = Sonic porosity.

Φ_d = Density porosity.

Effective Porosity:

Effective porosity is calculated by following formula

$$\Phi_s = \Phi_{\text{avg}} * (1 - \text{Volume of shale})$$

Calculation of Water Saturation (S_w)

To calculate saturation of water in the formation, a mathematical equation was developed by Archie given in equation given below.

$$S_w = \sqrt[n]{\frac{F \times R_w}{R_t}}$$

Where,

S_w = Water saturation.

F = Formation Factor ($F = \frac{a}{\phi^m}$).

R_t = True resistivity.

n = Saturation component value ranges from 1.8 to 2.5.

a = Constant value (with a constant value 1).

ϕ = Effective porosity.

m = Cementation factor (with a constant value 2).

Resistivity of Water (R_w)

Formation water resistivity (R_w) was calculated with the help of certain parameters like bottom hole temperature, surface temperature, water salinity in (ppm) and static spontaneous potential.

Calculation of resistivity of water (R_w)

For the calculation of resistivity of water following steps are followed

1. Read the SP value at the depth of maximum deflection, which gives SSP and is calculated by using the equation given below

$$SSP = SP_{\text{clean}} - SP_{\text{shale}}$$

Where,

SSP = Static Spontaneous Potential.

SP_{clean} = Spontaneous potential for sand.

SP_{shale} = Spontaneous potential for shale.

Values for the well Fimkassar-02 used, are given in the table given below

Table 4.4 Value of SSP, SP_{clean} , SP_{shale} for the well Fimkassar-02

SSP	SP_{clean}	SP_{shale}
-60 mv	0	60

2. Calculate the formation temperature (FT) from relation given in equation below at the depth of the SP value. Use Gen-6, (Schlumberger chart) given in appendix-1, with total depth and maximum temperature from the log header.

$$FT = \left[\frac{(BHT - ST)}{TD} \times FD \right]$$

Where,

FT = Formation temperature.

BHT = Borehole temperature.

FD = Formation depth (from surface to Fm).

ST = Surface temperature.

TD = Total depth (from surface to end).

3. Resistivity of mud filtrate (R_{mf1}) at surface temperature (ST= 26°C) is calculated using Gen-6 (Schlumberger chart) given in appendix-1, and it is 0.479 Ωm for well Fimkassar-02.
4. Calculate the resistivity of mud filtrate at zone of interest (FT) and it is calculated by equation given below

$$R_{mf2} = \frac{(ST + 6.77) \times R_{mf1}}{(FT + 6.77)}$$

Where,

R_{mf1} = Resistivity of mud filtrates at surface temperature (from well header).

ST = Surface temperature.

FT = Formation temperature.

R_{mf2} = Resistivity of mud filtrates at formation temperature. (R_{mf2} = 0.196 Ωm for Fimkassar-02).

5. Calculate Resistivity of mud filtrate equivalent (R_{mfeq}) at formation temperature, this is performed by considering the following, two conditions

- If R_{mf2} is greater than $0.1 \Omega m$ then correct it to formation temperature using the following relationship given in equation given below.

$$R_{mfeq} = 0.85 \times R_{mf2}$$

- If R_{mf2} is less than $0.1 (\Omega m)$ then use chart SP-2 (Schlumberger Chart) given in appendix-2 to derive a value of R_{mfeq} at formation temperature.

Calculation of Resistivity of water Equivalent (R_{weq}) and R_w

SSP is difference of maximum and minimum value of SP log. SSP is -60 mv and is plotted on Gen-6 (Schlumberger chart)

For True R_{weq} .

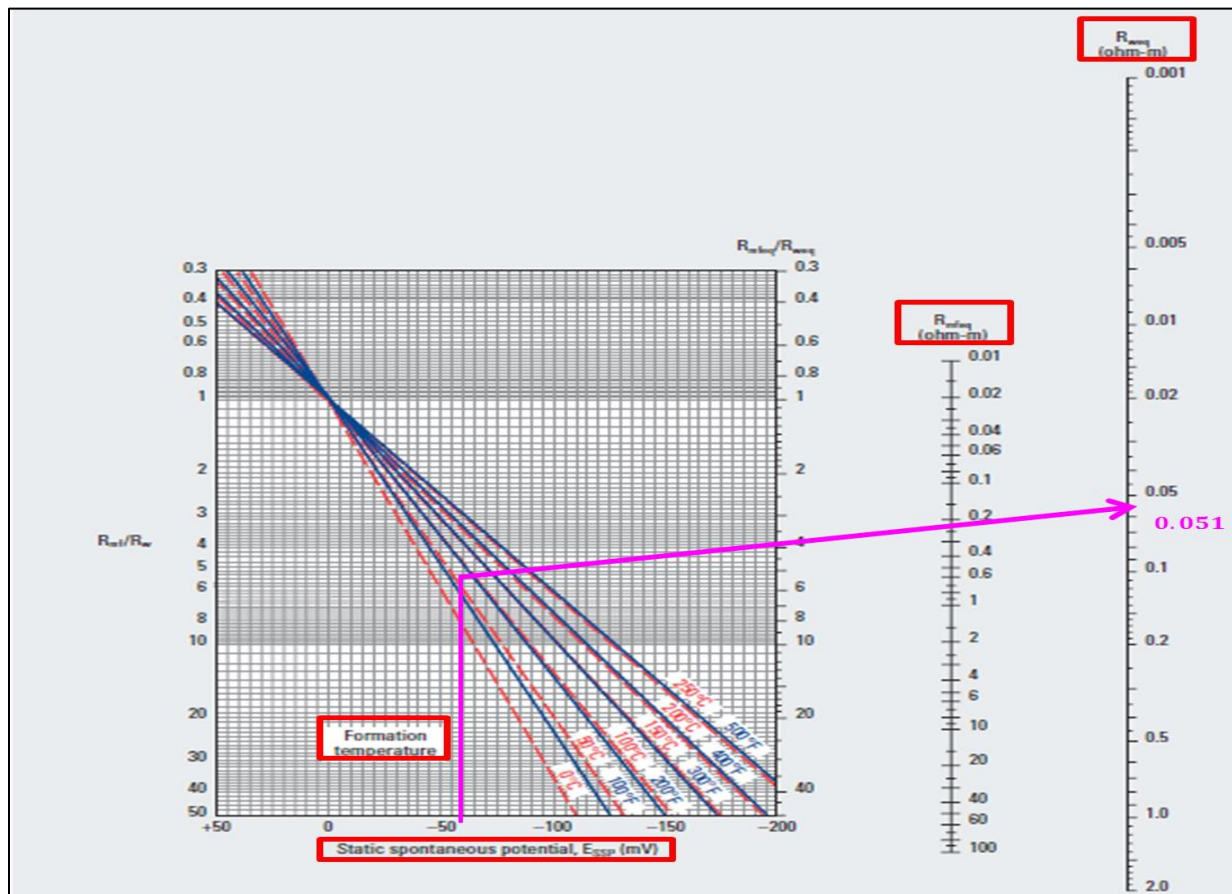


Figure 4.2 Determination of R_{weq} from SP chart (Schlumberger, 1989)

For True Rw

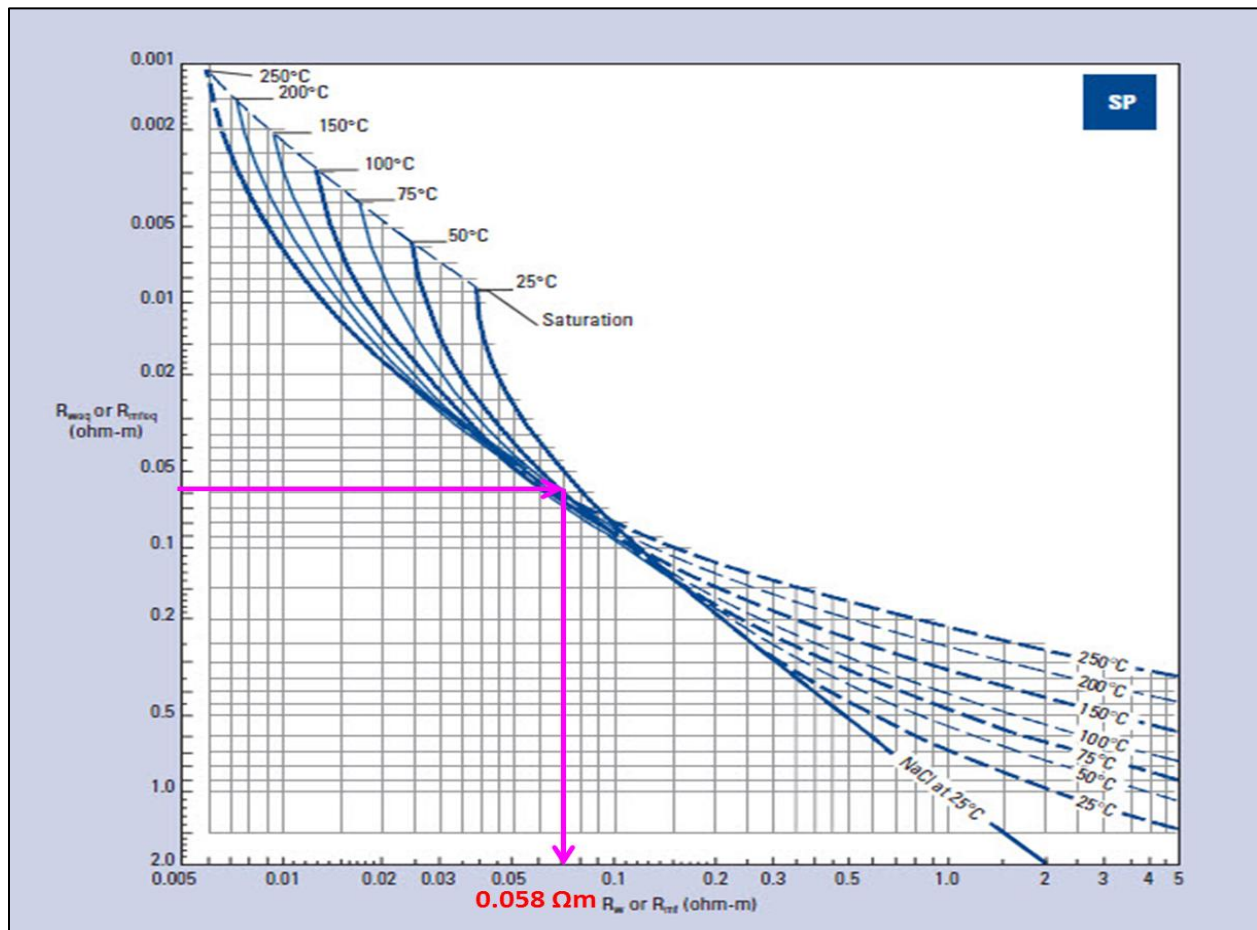


Figure 4.3 Determination of R_w from SP chart (Schlumberger, 1989).

Calculation of Hydrocarbon Saturation (S_h)

The fraction of pore spaces containing hydrocarbons is known as hydrocarbon saturation and is calculated by relation given in equation given below

$$S_h = 1 - S_w$$

Where,

S_h = Hydrocarbon saturation,

S_w = Water saturation.

As the S_h is the remaining percentage pore volume other than the percentage of pore volume occupied by water, hence this method is an indirect method which quantitatively estimate hydrocarbon saturation.

Well Log Interpretation of Fimkassar-02

Petrophysical analysis of Fimkassar-02 is done, based on the behavior of different log curves using SMT Kingdom (8.8). As a first indicator of lithology, GR log is very useful for the indication of shale. For the higher values of GR, higher will be the percentage of shale. Where there is low value of the GR shows less shale. Due to this reason, clean zone or shale free zones are defined easily, so it means that may be Hydrocarbon bearing zone is available. Resistivity logs are used to give the volume of oil/gas in a reservoir or in Petrophysical terms, to define the water saturation (S_w). When S_w is not 100%, then it shows hydrocarbons are present there. Higher the response of resistivity logs usually determines the presence of hydrocarbons or fresh water. Density mainly varies from 2.55 to 2.99 g/cm³ but somewhere at the reservoir level very high density corresponding to low resistivity is noted. It may be due to the Presence of some heavy minerals like gluconate, chlorite etc.

Criteria for marking the zone of interest

Criteria for marking the zone of interest is

- Low GR value.
- Caliper response must be smooth.
- Separation between LLD and LLS.
- Crossover between NPHI and RHOB.
- High effective porosity value.
- Low water saturation.
- High hydrocarbon saturation.

Petrophysical Analysis of Chorgali Zone

Only one main zone of interest is marked in Figure 4.4. Depth range of Zone of interest varies from 2905m-2915m in well Fimkassar-02 with a depth of 10m.

Shale volume of the whole depth range is 34 %. Effective porosity is about 7%, potential of the hydrocarbon is 42% and water saturation is 58%. This is only one pay zone in which high net pay is expected.

The reservoir properties for interested zone in Chorgali Formation is shown in Table 4.5.

Table 4.5

Average Volume of shale in %age	19%
Average effective porosity in %age	9%
Average water saturation in %age	51%
Average hydrocarbon saturation in %age	49%

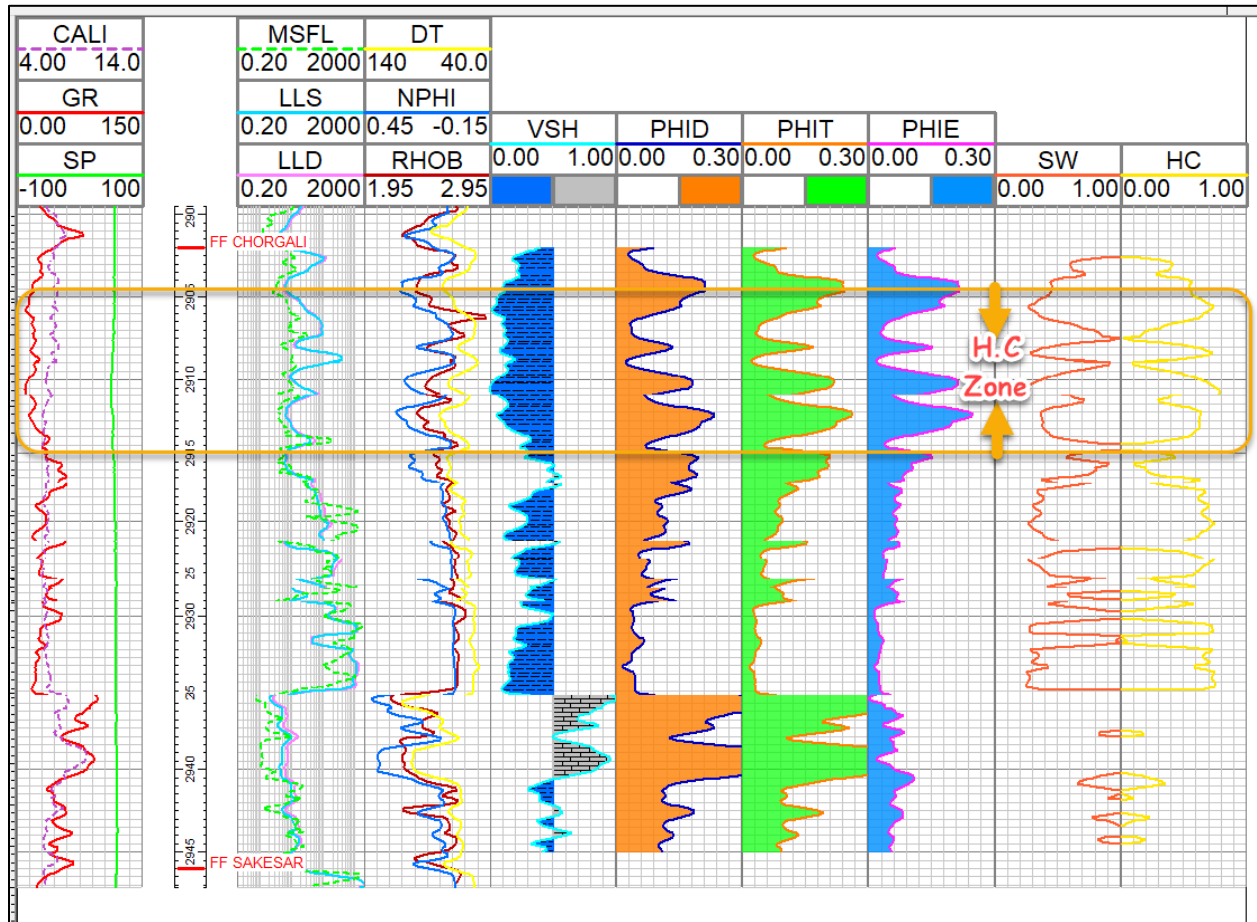


Figure 4.4 Petrophysical Analysis of Chorgali Formation.

Petrophysical Interpretation of Sakesar Formation

Petrophysical interpretation is carried out for Sakesar formation starts at a depth of 2950m to 2990m with a total thickness of 40m. Shown in Figure 4.5.

Shale volume of the whole depth range is 37 %. Effective porosity is about 2%, potential of the hydrocarbon is 41% and water saturation is 59%. This is only one pay zone in which high net pay is expected.

The reservoir properties for interested zone in Sakesar formation is shown in Table 4.6.

Table 4.6

Average Volume of shale in %age	21%
Average effective porosity in %age	2%
Average water saturation in %age	47%
Average hydrocarbon saturation in %age	53%

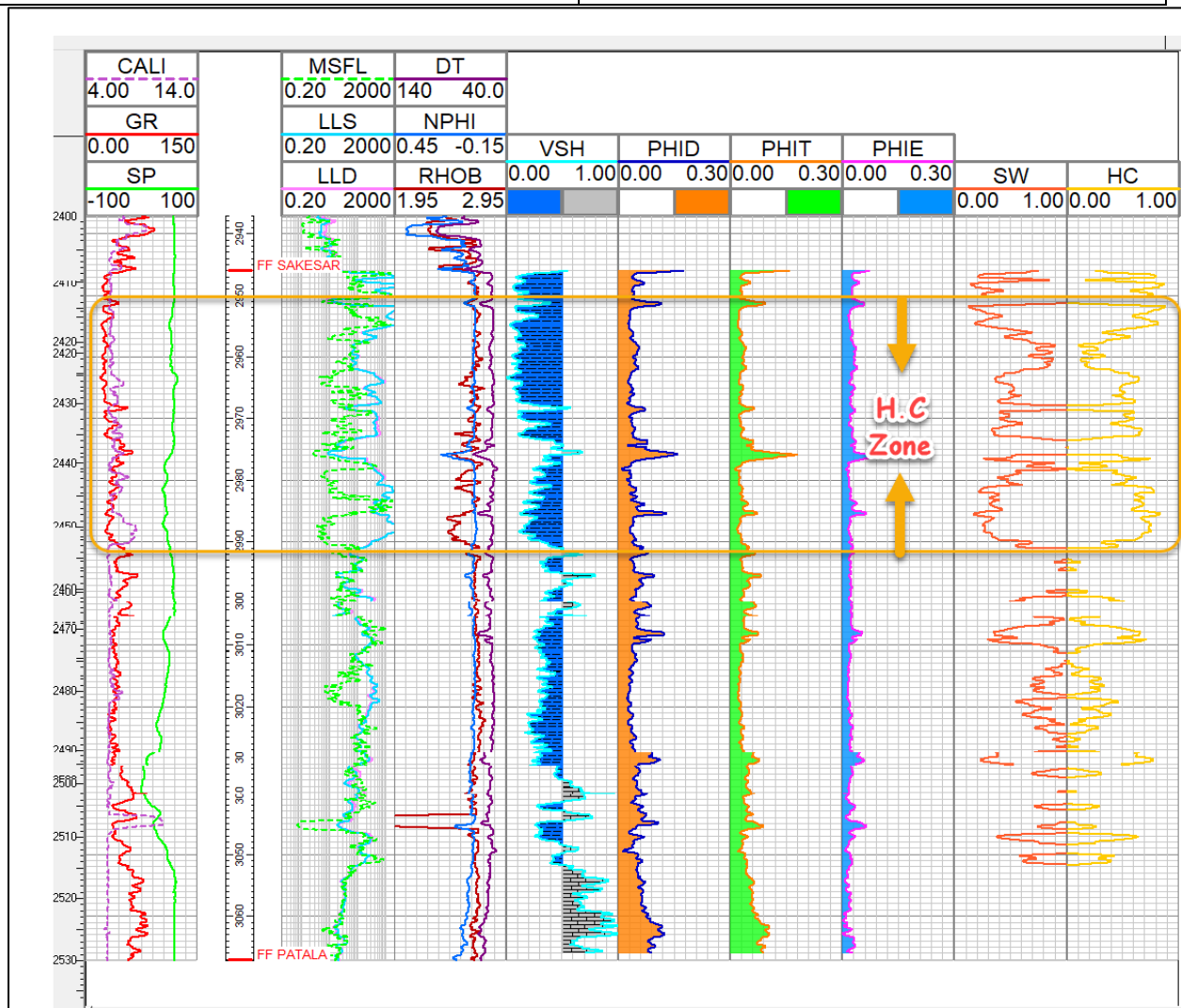


Figure 4.5 Petrophysical Interpretation of Sakesar Formation.

Chapter 5

Spectral Decomposition

Introduction

It is a process, that transforms seismic amplitudes as a function of space and time to spectral amplitudes as a function of frequency, space, and time. It yields very high resolution results (Wankui and Yanming, 2006). It is extremely helpful for seismic data interpretation by decomposing data into its spectral components and then reveals stratigraphic and structural details (Miao et al., 2007). It works on the principle of Fourier Transform and continuous wavelet transform etc. by transforming seismic data into frequency domain (Wie, 2010).

Methodology

The concept behind spectral decomposition is that seismic reflection from a thin bed has a characteristic expression in the frequency domain that is indicative of its thickness in time. A typical seismic trace contains information from multiple subsurface layers and just one single thin bed. The combine information from multiple subsurface layers usually results in complex tuned reflection, which has a unique frequency domain expression. To resolve these thin beds, spectral decomposition can be used (Partyka et al., 1999).

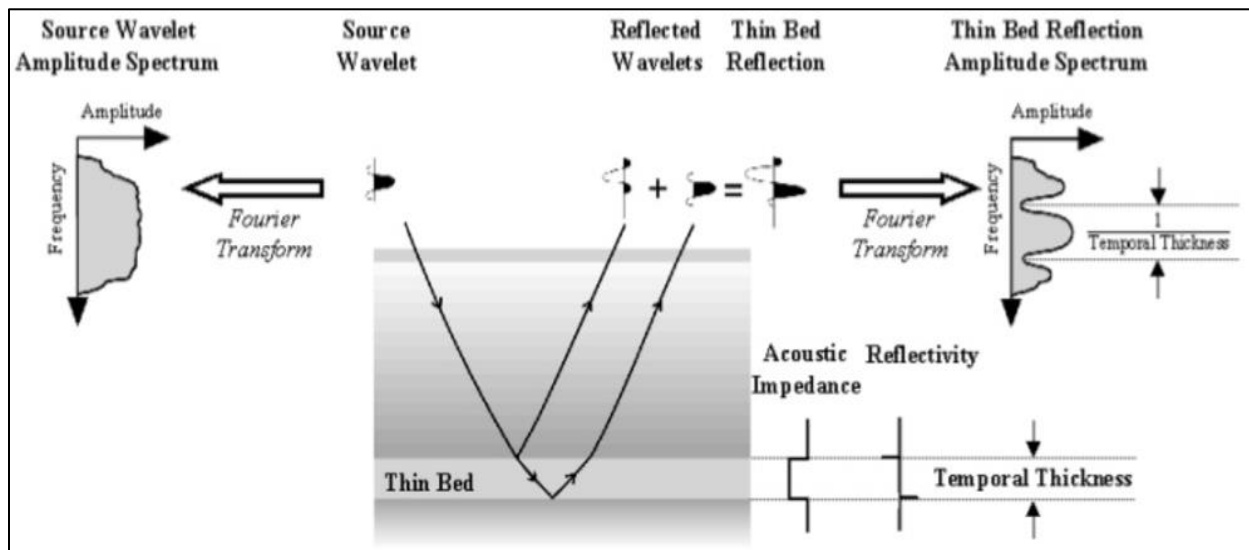


Figure 4.1 Spectral decomposition used to identify thin beds through analysis of the frequency spectrum in a short window around the time of bed (Partyka et al., 1999).

Comparison

A comparison is shown between the slices of spectral decomposition and amplitude slices of the seismic data. In these slices, we can see the enhancing resolution with the increasing Frequency. With this increasing resolution, we can see the minor details. A comparison is shown in Figure 4.2 between amplitude slice and spectral decomposition at 8, 10 and 13 Hz. We can see in these pictures that how the resolution is increasing with minor details.

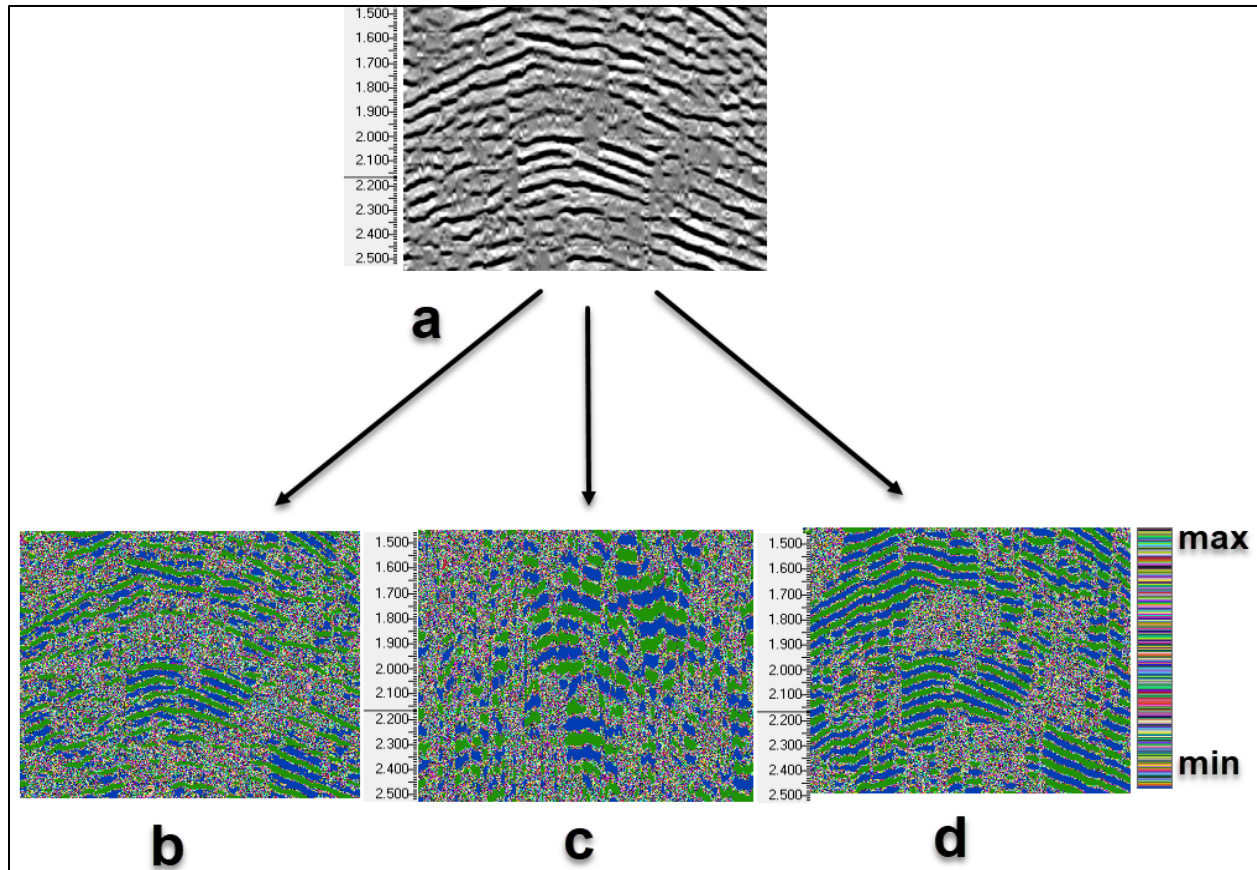


Figure 4.2 Comparison with seismic sections transformed by different spectral decomposition method. (**a**: Original seismic trace, **b**: Seismic section at 8 Hz, **c**: Seismic trace at 10 Hz, **d**: Seismic trace at 13 Hz).

Application of Spectral Decomposition

Spectral Decomposition is mainly useful in identifying

- Identifying minor faults.
- Identifying prospect hydrocarbon zones.

Identification of Minor Faults

Spectral decomposition is used to determine minor faults in seismic data. Figure 4.3 illustrates the seismic section with spectral attribute applied. Minor fault is marked at 17.2 Hz frequency.

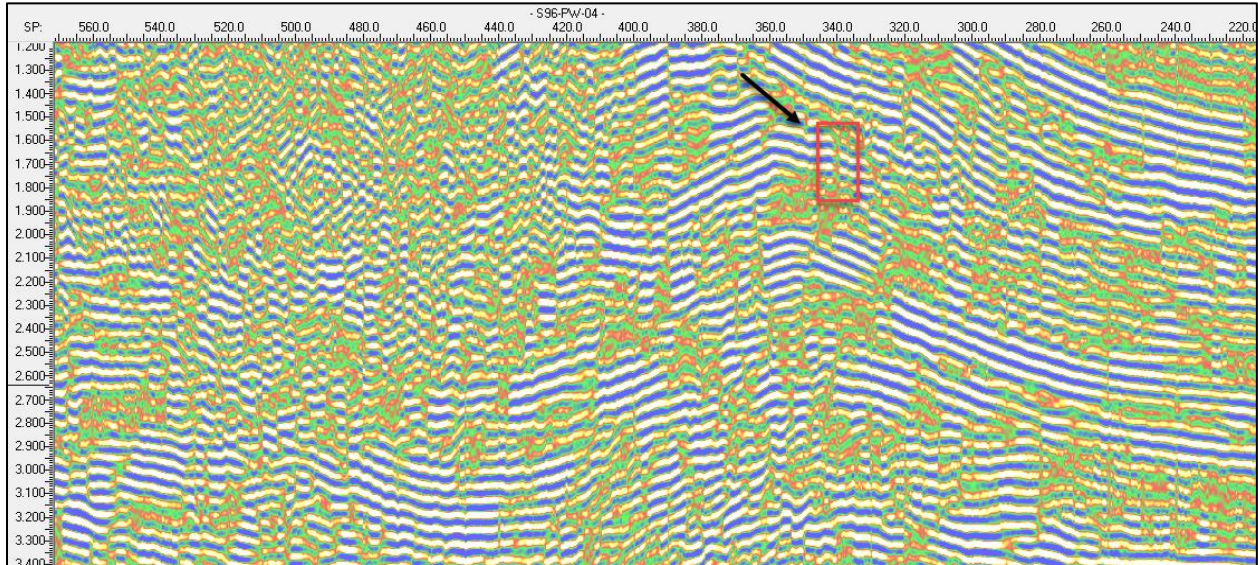


Figure 4.3 Section showing Minor fault at 17.2 Hz.

Identification of Hydrocarbon Prospect Zone

For the identification of Hydrocarbon prospect zones certain steps are followed, which are shown in Figure 4.4 in the form of a workflow.

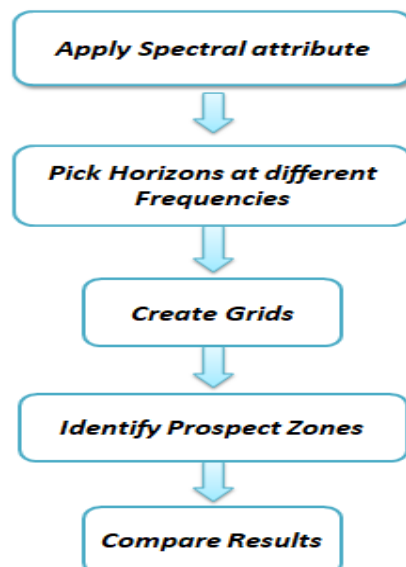


Figure 4.4 Workflow.

Comparison of Results

The results are compared at different frequency bands. The high amplitude anomaly shows the presence of gas while low amplitude is the indicator of oil in the reservoir. The frequency band of seismic data is 8-80 Hz. The bands of different frequencies created are 8, 10.2, 13.3, 17.2, 22.3, 28.8, 37.1, 48, 61.9, and 80 Hz. The results are compared at 8, 10.2 and 17.2 Hz.

Chorgali Grids

Figure 4.5, 4.6 and 4.7 show the results at 8, 10 and 17 Hz frequency respectively. The Hydrocarbon Zone is best available at 17 Hz. This can be explained by the color bar. This color bar shows the variation in amplitude. As the amplitude increases yellow or orange color appears. This yellow or orange colored area is our prospect zone.

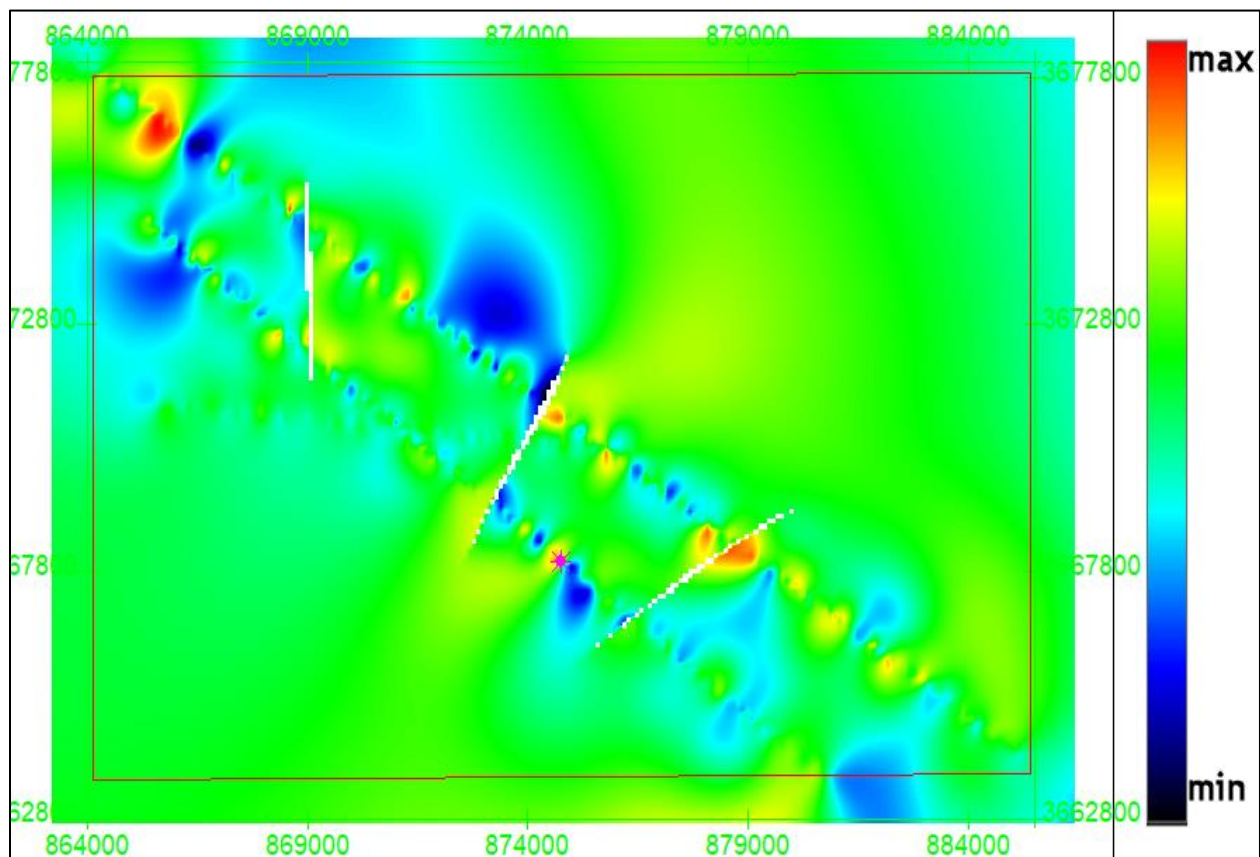


Figure 4.5 Chorgali grid at 8 Hz.

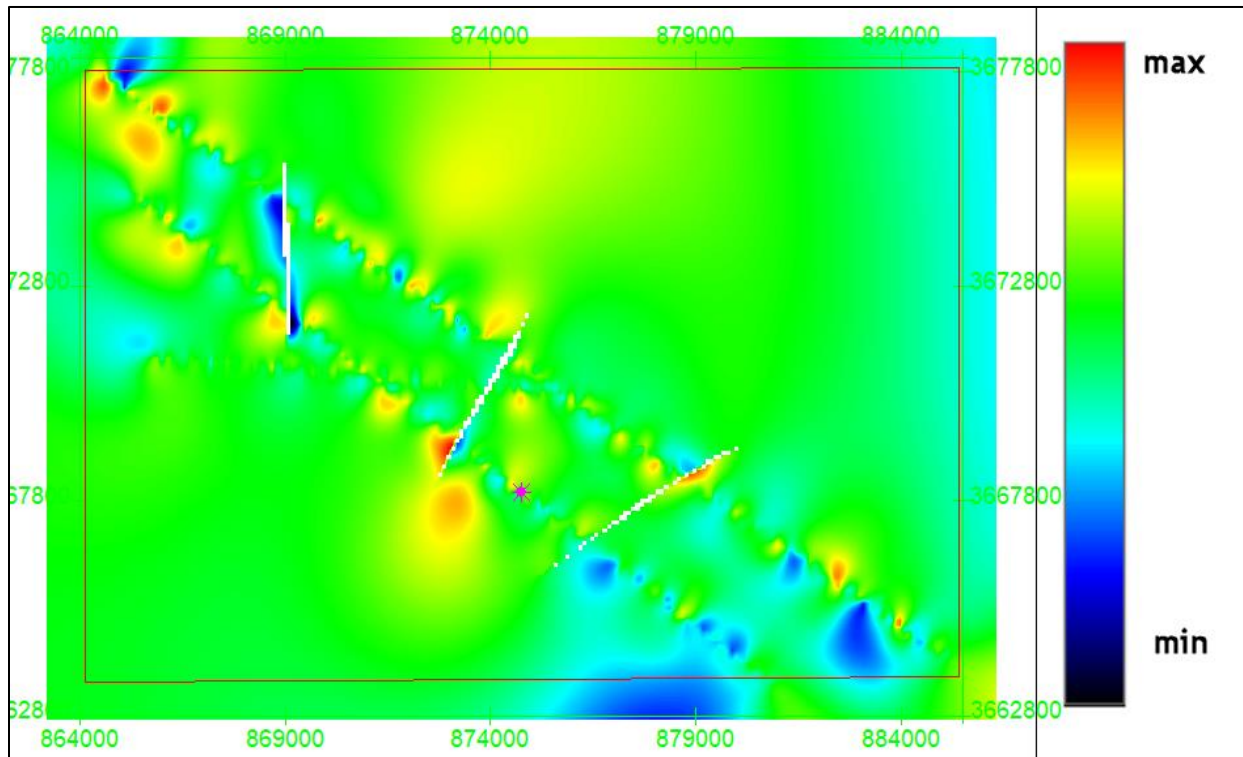


Figure 4.6 Chorgali grid at 10.2 Hz.

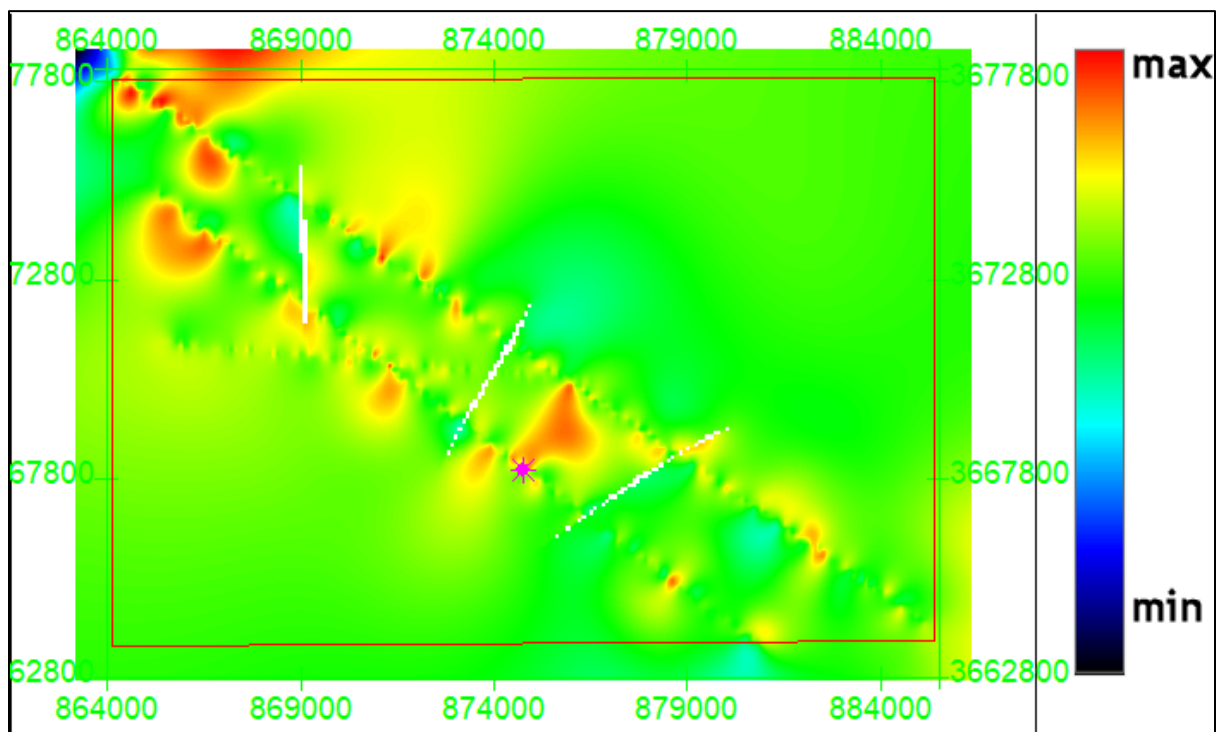


Figure 4.7 Chorgali grid at 17.3 Hz.

Sakesar Grids

Sakesar grids are marked at the same frequencies as in Figure 4.5, 4.6 and 4.7. Results are compared according to the color bar. Orange color denotes high amplitude.

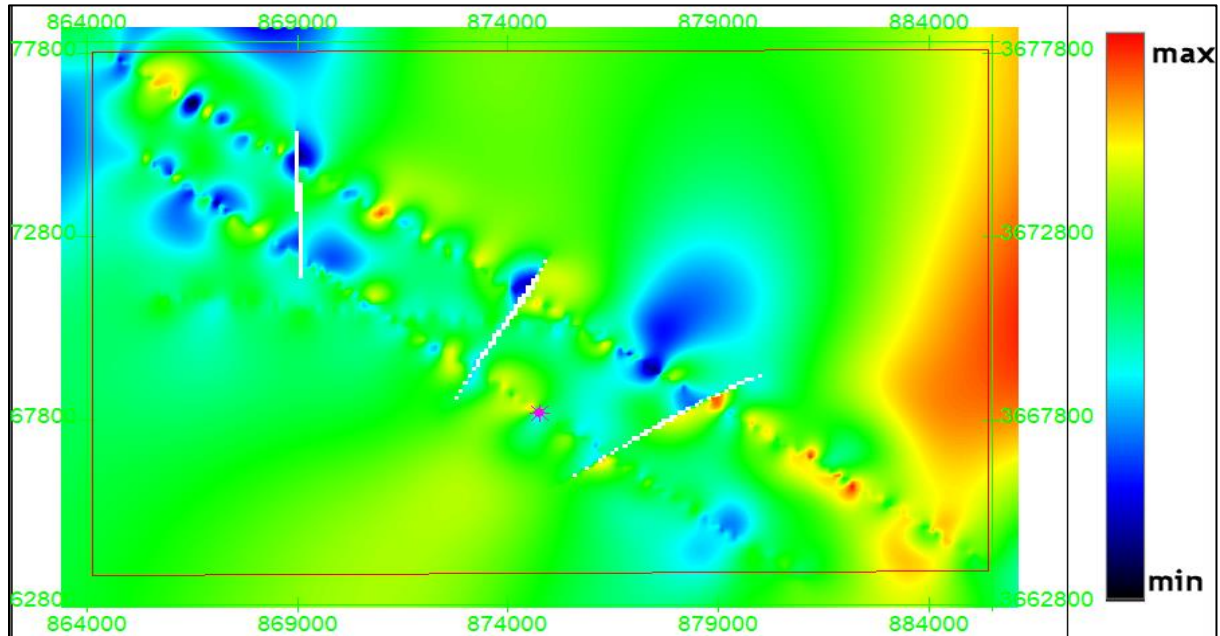


Figure 4.8 Sakesar Formation at 8Hz.

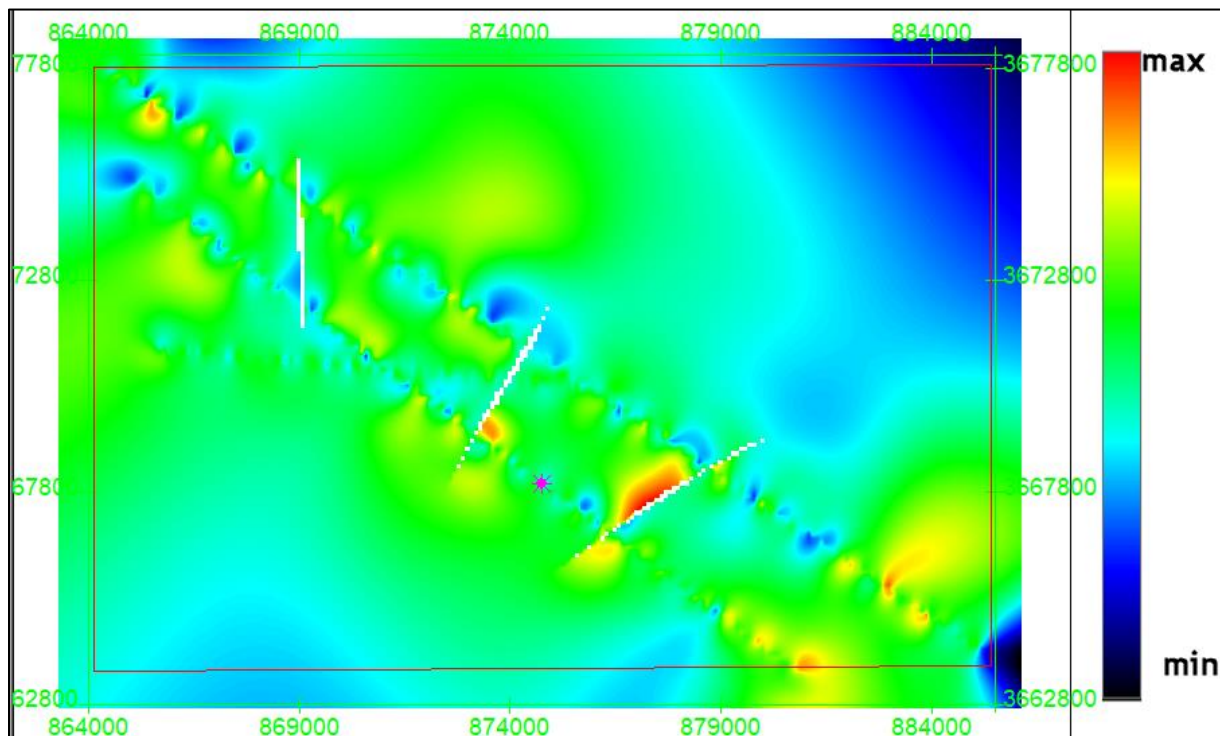


Figure 4.9 Sakesar Formation at 10.2 Hz.

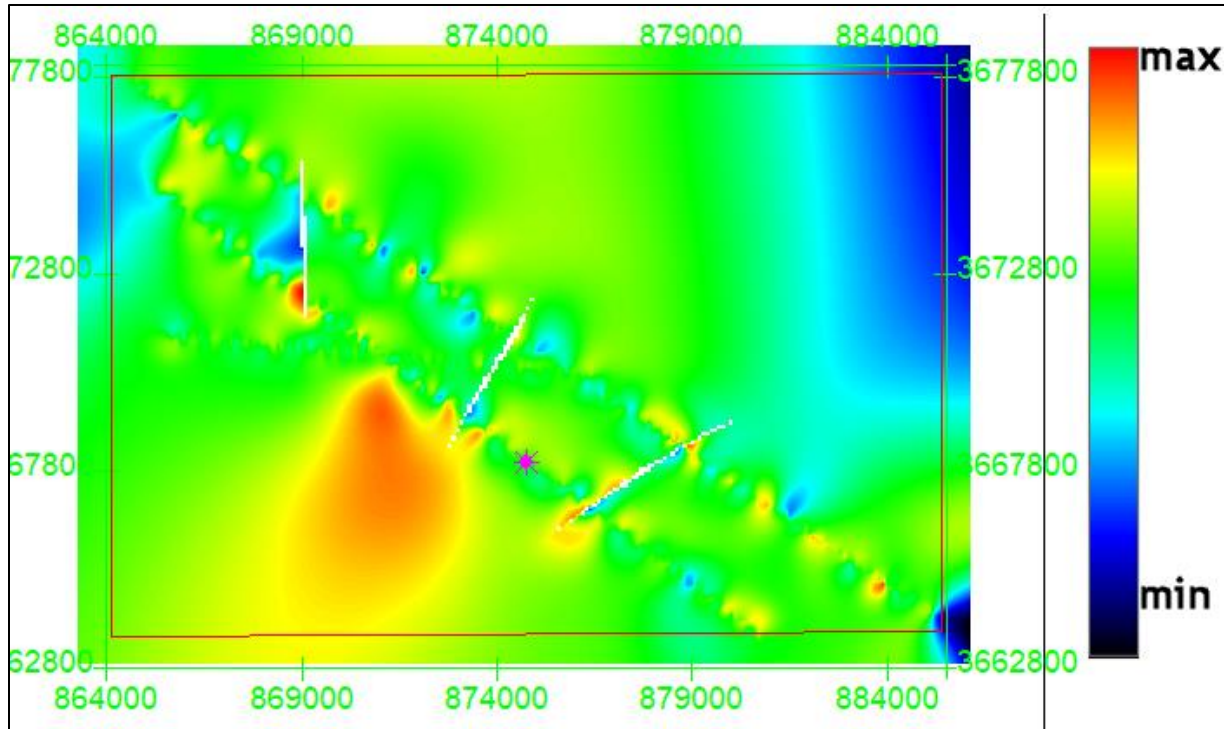


Figure 4.10 Sakesar Formation at 17.3 Hz.

In figures 4.8, 4.9 and 4.10 orange color denotes maximum amplitude. Blue color shows low amplitude. According to these colors we can mark our prospect zone.

Results & Conclusions

1. Seismic interpretation results have identified pop-up and snaked head structures in the area of study which are favorable structures for accumulation of Hydrocarbons.
2. On the basis of time and depth contour maps probable lead has been identified in the study area. These leads have been marked at Chorgali, Sakesar and Patala formation of Eocene level.
3. Due to limitation of data control, seismic attribute analysis only confirms the interpretation at some locations but do not give any reliable location to identify Hydrocarbons.
4. The petro physical interpretation of well Fimkassar-02 leads us to two probable zones for Hydrocarbon extraction one in Chorgali formation from 2905 to 2915m and second from 2905 to 2990m in Sakesar formation (act as reservoir rocks in the study area) respectively.

5. The results of spectral decomposition show a probable fluid saturation zone by decomposing the seismic amplitude at different frequencies. The response of seismic amplitude was checked at frequency 8, 10.2 and 17.3 Hz for Chorgali and Sakesar formation. At 17.3 Hz both the formations showed best response. This response was noted by high amplitude shown by yellow color.

References

- Aamir, M., & Siddiqui, M. M. (2006). Interpretation and visualization of thrust sheets in a triangle zone in eastern Potwar, Pakistan. *The Leading Edge*, 25(1), 24-37.
- Ali, A., Kashif, M., Hussain, M., Siddique, J., Aslam, I., & Ahmed, Z. (2015). An integrated analysis of petrophysics, cross-plots and Gassmann fluid substitution for characterization of Fimkassar area, Pakistan: A case study. *Arabian Journal for Science and Engineering*, 40(1), 181-193.
- Asquith, G. B., Krygowski, D., & Gibson, C. R. (2004). *Basic well log analysis* (Vol. 16). Tulsa: American association of petroleum geologists.
- Bacon, M., Simm, R., & Redshaw, T. (2007). *3-D seismic interpretation*. Cambridge University Press.
- Badley, M. E. (1985). *Practical seismic interpretation*.
- Bender, F., & Raza, H. A. (1995). *Geology of Pakistan*.
- Buxton, M. W. N., & Pedley, H. M. (1989). Short Paper: A standardized model for Tethyan Tertiary carbonate ramps. *Journal of the Geological Society*, 146(5), 746-748.
- Coffeen, J. A. (1986). *Seismic exploration fundamentals*.
- Dobrin, M. B. (1976). *Introduction to geophysical prospecting*. McGraw-hill.
- Ellis, D. V., & Singer, J. M. (2007). *Well logging for earth scientists*(Vol. 692). Dordrecht: Springer.
- Gee, E. R., & Gee, D. G. (1989). Overview of the geology and structure of the Salt Range, with observations on related areas of northern Pakistan. *Geological Society of America Special Papers*, 232, 95-112.
- Juggan, H., Abbas, G. (1991). On the Chogali Formation at the Type Locality. *Pakistan Journal of Hydrocarbon Research*. Volume 3, 35-45.
- Julián, C., Richard, P., Freddy, H., Williams, C., Raúl, C., Carlos, M., & John, C. (2009, January). The Use Of Seismic Attributes And Spectral Decomposition To Support The Drilling Plan Of The Uracoa-Bombal Fields. In *2009 SEG Annual Meeting*. Society of Exploration Geophysicists.
- Kadri, I. B. (1995). *Petroleum geology of Pakistan*. Pakistan Petroleum Limited.

- Kazmi, A. H., & Jan, M. Q. (1997). *Geology and tectonics of Pakistan*. Graphic publishers.
- Kemal, A. (1992). Geology and new trends for petroleum exploration in Pakistan. In *Proc. Internat. Petroleum seminar on new directions and strategies for accelerating petroleum exploration and production in Pakistan* (pp. 16-57).
- McQuillin, R., Bacon, M., & Barclay, W. (1984). An introduction to seismic interpretation-Reflection seismics in petroleum exploration.
- Miao, X., Todorovic-Marinic, D., & Klatt, T. (2007). Enhancing seismic insight by spectral decomposition. In *SEG Technical Program Expanded Abstracts 2007* (pp. 1437-1441). Society of Exploration Geophysicists.
- Nanda, N. C. (2016). *Seismic data interpretation and evaluation for hydrocarbon exploration and production: A practitioner's guide*. Springer.
- Partyka, G., Gridley, J., & Lopez, J. (1999). Interpretational applications of spectral decomposition in reservoir characterization. *The Leading Edge*, 18(3), 353-360.
- Sheriff, R. E. (2002). *Encyclopedic dictionary of applied geophysics*. Society of exploration geophysicists.
- Tittman, J., & Wahl, J. S. (1965). The physical foundations of formation density logging (gamma-gamma). *Geophysics*, 30(2), 284-294.
- Vail, P.R., Mitchum, R.M, and Sangree, J.B.(1997). Seismic stratigraphy and global changes of sea level, part 7; seismic stratigraphic interpretation procedure. *Seismic Stratigraphy Application to Hydrocarbon Exploration*. AAPG Memoir, 26,135-143.
- Wankui, G., Yanming, P., Rauch-Davies, M., & Yu, G. (2006). Successful application of spectral decomposition technique to map deep gas reservoirs. In *SEG Technical Program Expanded Abstracts 2006* (pp. 491-495). Society of Exploration Geophysicists.
- Wei, X. D. (2010, June). Interpretational Applications of Spectral Decomposition in Identifying Minor Faults. In *72nd EAGE Conference and Exhibition incorporating SPE EUROPEC 2010*.
- Yilmaz, Ö. (2001). *Seismic data analysis: Processing, inversion, and interpretation of seismic data*. Society of exploration geophysicists.

- Zerrouki, A. A., Aïfa, T., & Baddari, K. (2014). Prediction of natural fracture porosity from well log data by means of fuzzy ranking and an artificial neural network in Hassi Messaoud oil field, Algeria. *Journal of Petroleum Science and Engineering*, 115, 78-89.